Final Technical Report

U.S.G.S. - National Earthquake Hazards Reduction Program
Award 06HQGR0014

"Quaternary Fault Mapping and Quantification of 1906 Slip of the San Andreas Fault in Marin County, CA"

Project period: 12/01/05 to 12/31/07

Photograph of the 1906 San Francisco Earthquake rupture at the Skinner Ranch, Pt. Reyes National Seashore, Olema, CA (Bancroft Archives, University of California-Berkeley: BANC PIC 1989.060.1 24b)

Tina M. Niemi, Ph.D.
Department of Geosciences
University of Missouri-Kansas City
5100 Rockhill Road, Flarsheim Hall 420
Kansas City, MO 64110 U.S.A.
Tel: (816) 235-5342; Fax: (816) 235-5535; Email: niemit@umkc.edu

COSEISMIC DEFORMATIONS AND NEW SLIP ESTIMATES OF THE 1906 SAN FRANCISCO EARTHQUAKE RUPTURE ON THE SAN ANDREAS FAULT IN MARIN COUNTY, CALIFORNIA

Alexander Daehne and Tina M. Niemi
Department of Geosciences
University of Missouri-Kansas City
Kansas City, MO 64110, U.S.A.

Abstract

Soon after the 1906 San Francisco earthquake struck Marin County, geologists, notably G.K. Gilbert, mapped and measured structural damage and coseismic surface deformation generated by the rupture of the San Andreas Fault. In order to investigate and explain deformation patterns and to improve coseismic slip estimates recorded after the earthquake, we study published and unpublished reports and re-examine the locations where the effects of the 1906 earthquake were documented. We compare the historic information with recent field and remote sensing data. This enables us to detect morphological changes and to constrain more accurately the location of the 1906 fault trace. The recorded faults form complex deformation patterns and we propose a mechanism for the formation of subparallel faults linking mass wasting processes and distributed slip. The integration of historic and recent data enables us to better constrain the coseismic slip that occurred in 1906. An important aspect concerning coseismic slip is the great spatial variability implying that historic measurements were somewhat subjective and that the amount of measureable offset can greatly vary within a few meters. Analyzing the location of offset meander loops adjacent to the famous 6.1-6.4 m (20-21 feet) 1906 offset of Sir Francis Drake Boulevard (SFDB), indicates coseismic slip between 5.7 - 7.8 m. A 5 m coseismic slip estimate is reported from the Vedanta wind gap site and a topographic survey of remnants of a historic fence nearby yields an offset of about 7.4 m. Offsets greater than 6 m compare well to the slip calculated by geodetic models. Combining the findings on deformation patterns and coseismic measurements, we conclude that more than 6 m of 1906 coseismic slip is possible particularly across a wide shear zone, such as the SFDB.

1. Introduction

The San Andreas Fault (SAF) first gained the attention of California's citizenry, as well as that of the international scientific community, after the M_w 7.9 San Francisco earthquake of 18 April 1906. The rupture of approximately 500 km along SAF (Song *et al.*, 2008) (Fig. 1) devastated the city of San Francisco and inflicted widespread damage throughout much of coastal northern California (Boatwright and Bundock, 2005; 2008). Following the San Francisco earthquake, UC Berkeley Professor Andrew C. Lawson chaired the State Investigation Commission that assessed the earthquake rupture and damage to both man-made structures and the natural environment (Lawson, 1908).

The SAF in West Marin County is one of the largest undisturbed tracts of the fault in Northern California and thus provide us with a unique opportunity to study changes of the fault zone morphology over the past 100 years. The north and south portions of the SAF zone in

Marin County are submerged beneath the waters of Tomales Bay and Bolinas Lagoon but the transform fault crosses land through Point Reyes National Seashore Park, the Golden Gate National Recreation Area, and the Vedanta Retreat (Fig. 1). In this study we relocate published and unpublished historic photographs taken after the 1906 earthquake and collect new topographic data along the fault rupture in order to evaluate coseismic displacement and cumulative deformation along the SAF in Marin County.

Mapping the 1906 fault rupture and relocating archival earthquake photos is not only of historical interest. In the absence of long recurrence models for multiple segments of the SAF, coseismic slip and slip rate are often used to determine the rate of occurrence of earthquakes on a given segment. Understanding the slip distribution in the 1906 San Francisco earthquake or pre-1906 earthquakes is therefore a key parameter for estimation of earthquake probability models such as those presented in Working Group on California Earthquakes (WGCEP, 2003).

2. Geologic Setting

The SAF separates the Point Reyes Peninsula on the west from the North American mainland on the east (Fig. 1). Sharp bedrock contacts that produce linear surface expressions on both sides of the SAF valley (Clark and Brabb, 1997) suggest the existence of eastern and western boundary faults as first recognized by Galloway (1977). Although no recorded earthquakes are attributed to the faults, they are traceable in aerial images and Light Detection and Ranging (LiDAR) terrain models along the margins of the northwest-trending fault zone valley. Active tectonic geomorphic features such as sag ponds and disrupted drainages suggest that both the Eastern and Western boundary faults are active (Brown and Wolfe, 1972). The SAF Zone is dominated by late Pleistocene and Holocene deposition along the linear valley.

The Olema Valley is subdivided by a structural high at Five Brooks (Fig. 1). Along the southern part of the linear trough, shallow marine sediment of the Merced Formation (Pliocene-Pleistocene) lies within the fault valley and along the southern coast of Point Reyes Peninsula (Galloway, 1977; Clark and Brabb, 1997). Along the east side of Tomales Bay, the late Pleistocene Millerton Formation, composed of alluvium and estuarine deposits, outcrops and appears to correlate with similar deposit of the Olema Creek Formation, found in the northern-central part of the Olema Valley (Galloway, 1977; Grove *et al.,* 1995). Quaternary fluvial terraces cut into the margins of the Olema Creek Formation within the fault zone and into bedrock along margins of the SAF zone. Subsequent fluvial erosion dissected the terraces and deposited the eroded sediments in the center of the fault valley leaving topographic remnants referred to as 'medial ridges' (Hall and Hughes, 1980; Grove and Niemi, 2005). Marine terraces along the Point Reyes Peninsula record active uplift west of the SAF (Grove *et al.,* 2010).

3. Methods

3.1 Historic Photographs and Maps

Historic documents such as maps, photos, and sketches yield valuable information of specific sites because they reflect a contemporary state that can be compared to the modern landscape. We compare historic documents from various archival sources (Table 1) to recent observations from the same location in order to identify changes in the landscape and geomorphology. Our research was aided by published (Jordan, 1907; Gilbert, 1907; Lawson, 1908; Hall and Hughes, 1980; Wallace, 1980) and unpublished (Hall *et al.*, 1986; Livingston,

1993; 1995; Livingston, pers. comm., 2006) works for this region. During two field seasons in 2005 and 2006, we re-photographed 66 historic photographs by G.K. Gilbert, O.H. Wood, J.C. Branner, J.B. Macelwane, and unnamed authors from the Bancroft Archives. We obtained the absolute geographic position, the bearing of the field of view, and a modern digital photograph for each of the historic images. For all relocations we utilized a handheld Garmin 76CS, a Brunton Pocket Transit, and an Olympus Stylus 810 digital camera.

We also analyzed aerial photographs of the study area and georeferenced historic maps, including the 1862 U.S. Coast Survey map of a part of Tomales Bay, the 1916 and 1918 U.S. Coast and Geodetic Survey 15-Minute Point Reyes topographic quadrangle map, and the 1954 U.S.G.S. 7.5-Minute Inverness topographic quadrangle map that are available for download online. For our study of the channel meander migrations and changes in the marsh, we interpret aerial photographs from 1968 and 1982 for which the exact date and supplier are unknown. Both photographs have a scale of 1:10,000 and were scanned and georeferenced. We further use another dataset from the 1990s that was already available in digital format (see Table 1) and evaluate the accuracy of the dataset (see Electronic Supplement). The Marin Map Resource provided the highest accuracy of digital orthophotography for assessing fault traces, evaluating the accuracy of other aerial photographs, and georeferencing acquired maps and aerial images. The accuracy of this data set is a 0.3 m (1 ft) root mean square error (RMSE) in the horizontal, i.e., a randomly selected point is within 0.5 m (1.7 feet) of the true location on the ground at a confidence level of 95% (FGDC, 1998). Daehne (2007) and the Supplementary Data section of this paper provide a careful evaluation of all systematic errors and an accuracy assessment.

3.2 Survey Data, Processing, and Analyses

High-resolution topographic data provide an excellent tool for qualitative and quantitative analysis of ground deformation. In order to construct local digital elevation models of the 1906 rupture trace, we used Trimble R7 Zephyr Geodetic GPS antennae serving as real-time kinematic (RTK) base station and rover unit connected with a TrimMark 3 data radio link. Point observations with high (greater than 1m) RMSE were removed from all surveys using surveying software (see Supplementary Data). We also corrected survey coordinates by comparing ground control coordinates to points on Digital Orthophoto Quarter-Quadrangles (see Supplementary Data). Due to the divergence of the GPS receiver-derived autonomous elevation from the actual sea level, we adjust observed elevations using USGS 24,000-scale digital elevation models (DEM) that are available online.

For the post-processing of survey data and manipulation of spatial information, we used ESRI's Spatial Analyst geostatistical methods of kriging and inverse distance weighting to interpolate topographic surfaces and image offset preserved in the geomorphology. We try to minimize the software-predicted error for these spatial interpolations by adjusting the model parameters. By comparing calculated models resulting from different input values with respect to their error prediction and fit to a triangulated network surface, we find that in both kriging and inverse distance weighted computation the default values calculated by Spatial Analyst provide sufficient accuracy.

However, using the method described above to match displaced contours across the fault has some limitations. It assumes offsets occur solely in the form of lateral displacements.

Thus, vertical displacements of a slope surface can create a bias in the measurable horizontal offsets. Secondly, quantitative measurements of offset are manually obtained by measuring displacement of a contour line along a defined fault plane. We minimized the error introduced through the model by using historic documents to evaluate the displacement. Furthermore, we rely on two different geostatistical models and measure offsets from multiple piercing points (i.e. using multiple contour lines).

4. Deformation and Offsets along the 1906 Fault Trace

In this study we focus on the SAF along the north and central portion of Olema Valley (Fig. 1). In the following section, we describe data from north to south: Tomales Bay, Sir Francis Drake Boulevard (SFDB), the meander loops of Bear Valley Creek, Silver Hills, Point Reyes National Seashore Headquarters (Skinner Ranch), and the Vedanta Retreat (Shafter Ranch) (Fig. 1).

4.1 Tomales Bay

Tomales Bay is a 1.4 km wide elongated bay that connects the Pacific Ocean with the delta and tidal marsh of Lagunitas Creek (also know as Papermill Creek). Lagunitas Creek enters the head of the bay from the east and flows west towards the western margin of the bay (Fig. 2a). There, the stream makes a meander loop reorienting its course towards the north. At about one km to the north the creek and the fault trace intersect, and the creek thereafter parallels the rupture. The 1906 mole track photographed by Gilbert (Lawson, 1908) itself is no longer preserved because the head of the bay underwent major modifications in the 1930's when low-lying areas were converted to pasture by the construction of several levees and a dam (Livingston, 1995; Niemi and Hall, 1996).

The location of Lagunitas Creek allowed us to compare G.K. Gilbert's sketch (Fig. 2b in this paper and Fig. 24 in Lawson, 1908) to a basemap, a georeferenced 1916 United States Coast and Geodetic Survey topographic map (1:62,500). This map was scanned and georeferenced using a current USGS topographic map (1:24,000). We identified 53 locations suitable for georeferencing, mostly consisting of benchmarks and spot elevation markers. These locations are consistent in both maps, and produced an acceptable error (RMSE approximately 38 meters). Evaluation of the historic topographical map of 1916, in conjunction with historical photographs (Fig. 2c), G.K. Gilbert's sketch of Tomales Bay (Fig. 2b), and geomorphic lineaments on aerial images, allowed us to precisely map Quaternary faults within Tomales Bay. We estimate the accuracy of the marked fault trace to be equivalent to the above reported RMSE value of 38 meters produced by georeferencing.

The 1906 fault trace lies slightly to the west of the middle of Tomales Bay and subparallel to the east and west boundary faults (Fig. 2a-c). G.K. Gilbert (Lawson, 1908) described in detail the expression of the earthquake rupture trace propagating through the gently sloping terrain of the delta of Lagunitas Creek towards the estuary. Furthermore, Gilbert produced a sketch map (Fig. 2b) of the bay showing the 1906 fault trace striking more easterly than the Tomales Bay margins.

Figure 2a is a comparison between fault mapping by Brown and Wolfe (1972), Alquist-Priolo Fault Zoning Act (California Geological Survey (CGS), 2001) and our own research. Figure 2 shows that Quaternary fault traces we map are similar to previous fault and geologic maps

(Brown and Wolfe, 1972; Galloway, 1977; Clark and Brabb, 1997, California Geological Survey, 2001; Bryant, 2005). On the basis of supporting evidence found in aerial images, the west boundary fault, first mentioned in Galloway (1977), is better located close to the western margin of Tomales Bay. Air photos also provide evidence for inference that the east boundary fault that is documented by CGS as far north as Olema, extends parallel to the eastern margin of Tomales Bay (Fig. 2a), north of Point Reyes where the fault runs partially parallel to a railroad embankment.

4.2 Sir Frances Drake Boulevard Offset

The maximum measured surface slip in the 1906 earthquake is the 6.1-6.4 m (20-21 ft) (Lawson, 1908) offset of Sir Francis Drake Boulevard (SFDB, also known as the Levee Road; Fig 3a, 3b) across the head of Tomales Bay, 0.8 km west of Point Reyes Station.

> G.K. Gilbert writes (Lawson 1908: page 71):
> *The road running southwest from Point Reyes Station and crossing the valley at the head of Papermill Creek delta was offset 20 feet. (Fig. 23 and plate 47 B). As the fault-trace at this point was between 50 and 60 feet wide, and as the embankment of the road for that distance was broken into several pieces, it was not possible to make certain that the dissevered remnants of the road had originally been in exact alignment. It is probable, however, that the road was approximately straight before the earthquake, and that the exceptionally great offset at this point is to be explained as the result of a horizontal shifting of the surface materials. The embankment of the road rested on marshy ground so soft that a portion of the embankment sank into it, and material of this character was in other localities demonstrably shifted.*

> W.W. Rubey writes in Lawson (1908) on page 148:
> *The horizontal displacement on the fault, as measured on fences, roads, and various structures which cross the fault-trace, is also apparently quite variable, ranging from a foot or less up to 20 or 21 feet.*

A modern measurement of the SFDB at this location is difficult because of modifications in the past century. There are no detectable signs of the 1906 offset apart from an extant fence along the road west of the fault. In spite of the upgrading and expansion of the historic 1906 road, the offset was still visible in 1928 when Father James Bernard Macelwane visited the site (Figs. 3e and 3f). Careful relocation of the historic photograph sites indicates that the road west of the fault zone was originally located farther to the north of today's SFDB.

To uncover the original location of the SFDB, we used a historic fence post (compare to Fig. 4) that we discovered to determine both the road's changed position and for an independent measure of coseismic slip in the 1906 earthquake. The photographs of the SFDB (Figs. 3c-3f) show a fence along both sides of the road. We observe from Gilbert's post-earthquake photographs (Figs. 3c and 3d) that the northern fence seems to be better maintained than the southern one that remained damaged after the earthquake. This supports our interpretation that the post we discovered was part of the historic northern fence that can be seen in Figures 3c and 3d. Unfortunately, no historic offset measurement document the

fence offsets even though Gilbert sketched the fence in his field notes (Notebook 108, Saturday, April 28, 1906).

We can use Gilbert's exceptionally detailed sketch to describe the fracture pattern across the fault zone and to estimate the offset of the road (Fig. 4). Digitizing and referencing this sketch with ArcGIS is only possible with some necessary assumptions that can help to derive reference coordinates (see Supplementary Data). From Gilbert's notes and Lawson (1908), we know that the width of the fault zone was determined to be 15-18 m and the offset across the fault about 6 m. From historic photographs we approximate the width of the wheel tracks to be about 2 m. We also know that the general trend of the fault zone is about 325˚. Another clue is provided from Figures 3d and 3f. A culvert that is clearly visible in the foreground of the Gilbert photo (Fig. 3d) is not on the fault zone sketch (Fig. 4). We estimate that there is at least 20 m between the culvert and the edge of the SAF shear zone. Based on these interpretation, we georeferenced and digitized the sketch (Fig. 4). From our reconstruction, we estimate offset of SFDB to be about 6.5 m. Determining the accuracy of this estimate remains somewhat subjective. However, after using all of the above-mentioned contributing values in a georeferencing table, the computed RMSE values of six carefully chosen locations total about 0.6 m, which is an approximation of the accuracy of the mapped features.

At the SFDB location the fault trace is not a single strand, but rather is an approximately 20-m-wide zone that accommodated about 1 m settling that G.K. Gilbert ascribes to lateral spreading of the embankment (Fig.4). The georeferenced image of G. K. Gilbert's sketch (modified from Lawson, 1908) (Figure 4) shows the fracture pattern observed on the SFDB dirt road following the earthquake. The bridge covering the culvert, as seen in Figure 3d indicates that a small stream that drains the Marsh into Lagunitas Creek flows into immediate vicinity of the fault trace. Thus, we conclude that the road's embankment is essentially resting on saturated alluvium. Riedel and P shears are clearly identifiable in the sketch and give an excellent example for a right-lateral shear zone. The dominant fractures are synthetic Riedel shears (R shears), transtensional fractures that develop at low angles to the shear zone margins (e.g. Tchalenko, 1970; Wilcox, 1973), and that trend roughly 15˚ to the main fault trend. Conjugate Riedel shears (R') are missing, whereas some P shears were observed. We ascribe lateral spreading and settling of the unconsolidated embankment as transtensional dextral shearing that creates tensile stresses.

4.3 Bear Valley Meander Loops

Analyses of the 1862 coastal map (Fig. 5) and aerial photographs of the marsh (Fig. 6), reveal repeated faulting of Bear Valley stream meanders. We registered the historic coastal map using its original coordinates and calculated an RMSE of about 25 meters (see Electronic Supplement). We then compared the historic coastal map with more recent orthophotographs (from the years 1966, 1982, 1990s) and identified topographic features. We found that a meandering creek joining Lagunitas Creek from the south identified on the 1862 map remained traceable on orthophotos over 100 years later.

For each individual image, we mapped locations and possible fault deformation of the meanders, streambeds, and oxbow lakes. For example, when a stream crosses a strike-slip fault the stream becomes deflected and eventually the upstream channel segment is captured by a segment located downstream of the fault (Schumm *et al.* 2000). We found that three

meanders within the marsh were clearly crossed by the 1906 fault trace causing the meanders to bend sharply at the fault and to display incremental movement towards the northwest, rather than gradual lateral migration to the northeast.

Furthermore, the meanders show large scale, long-term deformations along the fault trace. The largest offset, traced on two of the three aerial photographs, was determined to be 44-50 m (Fig. 6A and 6B). Characteristic of this particular site today is a relatively linear creek bed along the eastern margin of the marsh, which in 1862, still formed a meander to the west followed by a number of bends before it joined Lagunitas Creek (see Fig. 5). Many of the abandoned meanders along the eastern margin of the marsh branching off to the west show an offset where they are traversed by the fault. Furthermore, the high curvature observed in the meander loops is unexpected for undeformed streams and is categorized by Schumm *et al.* (2000) as R4-class right-lateral deflection.

The 1906 fault trace can be identified on the basis of the sharp angle of the meander bend where the creek crosses the SAF. This is atypical and suggests that the natural fluvial processes are too weak to erase the signature that co-seismic displacements left in the meanders. Normally, channels adjust after strike slip by gradually decreasing the deflection of the channel that over time increases the radius of the arc of the meanders (compare to Schumm *et al.*, 2000). We found this in at least one location at the southeast corner of the marsh where a small offset is preserved and erosional processes are not able to fully erase the displacement history.

Wallace (1968) proposed that the minimum channel displacements recorded might represent the latest slippage. Consequently, we are able to distinguish the location of the 1906 fault trace on the air photos where we discovered the most recent offsets preserved at the southern end of the meander loop. Comparing the three aerial images (Figs. 6a-c), we measure corresponding offsets of the identical feature ranging from 5.7 ± 0.6 m to 7.8 ± 2.4 m. The reported accuracy is computed using the RMSE of the georeferenced basemap and calculations for computation of circular standard error at 95% confidence within accurate location, as defined by the Federal Geographic Data Committee (1998). Immediately after the 1906 displacement, the stream likely started to counteract the atypical meander morphology by degrading the curvature and eroding along the cutbanks. Therefore, an unknown portion of this offset may be attributed to fluvial erosion. On the other hand, the offset meander loop may record cumulative slip from two earthquakes. This site holds promise for further paleoseismic investigations although it is currently inaccessible because of the thick vegetation in the marsh environment.

4.4 Silver Hills

Approximately 600 m southeast of SFDB, the 1906 fault trace runs along the western slope of a medial ridge commonly referred to as Silver Hills (Dewey Livingston, pers. comm. 2006, see Fig. 7a). South of Tomales Bay the fault traverses these hills for a distance of about 1820 m to a marsh north of the headquarters of Point Reyes National Seashore. G. K. Gilbert (in Lawson, 1908) described the surface expression of the fault trace as forming small ridges, approximately 0.9 m – 3 m wide and only a few centimeters to 0.5 m high. These low elevation ridges, that are now commonly called the mole track, trend mostly parallel to the margins of the fault zone and can be found throughout the valley between Tomales Bay and Bolinas

Lagoon. The higher ridges within the valley (medial ridges) extend up to 5 km in length and up to 50 m in height (Hall and Hughes, 1980). Their origin is not fully understood, but might be related to either transpression (Wallace, 1949), or displacement of alluvial fans, or both (Hall and Hughes, 1980). Galloway (1977) and Grove *et al.* (1995) mapped folded and tilted upper Pleistocene units within the medial ridges. Grove and Niemi (2005) reported slip rates of 17-35 mm/yr for the SAF based on offset of the Olema Creek Formation from its source rocks on Inverness Ridge to the west and ~25 mm/yr based on displacement of late Pleistocene alluvial fan deposits from its source drainage.

We investigated the active tectonic geomorphology of one of the medial ridges, Silver Hills. Figures 7, 8, and 9 summarize the complex deformations across multiple subparallel-trending fault traces evident in the geomorphologic expression of the ridge. Air photographs, LiDAR data, and field investigations provide the basis for the mapped fault locations. In the northern portion of the Silver Hills which extent parallel to Bear Valley Road, Gilbert photographed a ridge slice that was noticeably offset and where the 1906 fault rupture was apparently confined to a single fault trace (Figs. 7b, 7c, and 8a). Only 350 m farther to the north, another site is characterized by distributed shear and large-scale cumulative offset documented by historic photographs by Macelwane (Fig 7e) and a distant photograph by Gilbert. Gilbert did not record or photograph in more detail the ridge spur shown in Figures 7d, 7e and 8b which lies upslope of the main fault trace. However, a few available photographs from more distant vantage points suggest that also this part experienced offsets during the 1906 earthquake.

Where contour lines cross a strike-slip fault, they show distinct signs of displacement in that they are deflected from the natural geomorphologically determined, ridge-parallel course towards a fault-parallel course (compare Figs. 7b, 7c, 8a, and 8b). This fault-parallel course in the contour lines can be measured and seen as an estimate of the amount of horizontal offset along the fault trace. For this purpose we used both kriging (Figs. 7b and 7c) and inverse distance weighted surface models (Figs. 8a and 8b) to measure offset. We report the results (see Supplementary Data) for each measured topographic contour line individually. To estimate the accuracy we compute the sum of RMSE errors contributing to the computation of the results, namely survey accuracy, statistical model accuracy, and the range of measurements. We reported the error as the median of the calculation above.

The main limitation of this method is that we have to assume that displacements are confined to horizontal slip. Although Gilbert indicated oblique slip in many locations, the captions accompanying the photograph in Figure 7c indicate that he observed mostly right-lateral, strike-slip motion. Right-lateral translation of the topographically higher part of the ridge has produce the apparent vertical offset and the northeast-facing fault scarp. In the captions accompanying two photographs (Gilbert photo numbers 2843 and 2926, USGS photographic Library, see Table 2), Gilbert clarifies that the “apparent upthrow is chiefly due to the combination of horizontal throw with slope.” Faulting at this location is confined to a single narrow trace and has translated the ridge slice by 7.5 $\pm$ 0.7 m (Figs. 7b, c and 8a). Our measurements is nearly double the observation of 13.5 feet (4.1 m) of coseismic slip reported by Gilbert (Notebook 108,Thursday, May 10, 1906), suggesting it might represent cumulative slip in more than one earthquake similar to one of the Bear Valley meander loop measurements.

Farther north at the Silver Hills, the slip history is not well enough constrained because the active fault traces were not sketched in detail or described after the 1906 earthquake. However, Hall and Hughes's (1980) interpretation of one of Gilbert's photographs reveals that the trace did indeed experience displacements. During our field research and studies of published and unpublished data we discovered geomorphic evidence for at least three, possibly even four fault traces in some areas the ridge. A photograph by Macelwane, who visited the area in 1928, shows a view of the ridge, dissected and displaced by two active traces (Fig. 7d). Both photos (Figs. 7c and 7d) illustrate the complex active fault scarp morphology at the Silver Hills. Gilbert's field notes do indeed confirm that he observed smaller offsets here compared to what he recorded at the southern offset ridge slice or at the headquarters of Point Reyes National Seashore (Skinner Ranch), and further notes that the fault movement is not confined to a single fault trace.

> Notebook 108,Thursday, May 10, 1906;
> *2 m [miles] north of Olema I photoed the fault where vertical throw is shown. The indicated amount is 22". The horizontal throw at the same place is 13.5 feet. A half-mile farther north on a knob of the hillside, the throw seems to be only 2 – 3' hor. (horizontal) and half as much vertically. The slickensides dip 28° to SE. This is not the whole of the fault. There are several subparallel faults up the hill and one of them shows a hor. (horizontal) throw of 1 ft.*

Gilbert measured vertical offset from southeast-plunging slickenlines farther to the north and might be attributed to the failing slope during the earthquake (Figures 7d, 7e and 8b). Hall and Hughes (1980) confirm this and suggest that the atypically high vertical separations, as well as the aberrantly low horizontal displacements originate in coseismic and seismically-induced landslides. Hall and Hughes (1980) mapped branching fault traces, as well as sag ponds, both of which occur throughout the area.

Through aerial photo interpretation and LiDAR data analysis, we identified and mapped the 1906 rupture trace and other Quaternary fault traces at the Silver Hills ridge site (Fig. 7a). Following Gilberts observations we infer that seismically-induced, vertical offsets are small enough to allow for measurement of offset topography based on simple shear. Conversely, this yields only information on long-term deformations rather than a well-constrained measurement for a singular event due to the aforementioned limitations of the computation of offset contours. We estimate the cumulative displacements from multiple events along a subparallel branch of the 1906 fault trace yield a measurement of 17 $\pm$ 2.2 m of lateral offset (Figs. 7d and 8b). This measure indicates a long deformation history recording at least four earthquakes considering Gilbert's field measure (4.1 m) detected after the 1906 earthquake on a single trace 400 m farther to the south (Figs 7b,c, 8a).

Based on our own observations, we concur with Hall and Hughes (1980) that complex landsliding greatly impacts the historic and current morphological expression of the Silver Hills and propose a model that links coseismic deformations and mass wasting processes (Fig. 9). Some of the spatial variations in slippage documented G.K. Gilbert's notebooks (4.1 m of slip at one point and only 0.6 m – 0.9 m at a location 800 m farther northwest) can be attributed to slip partitioning between multiple strands (0.6 m-0.9 m on one strand and an additional 0.3 m on another). These subparallel-trending branch fractures of the main trace constitute a

structurally weakened zone along the western flanks of the Silver Hills medial ridge. The unconsolidated alluvial and colluvial sediments that comprise the ridge (Hall and Hughes, 1980) do not support the seismically-induced, over-steepened slope angle. Gilbert's description of vertical throw and slickenlines indicate oblique slip on the faults that trend sub-parallel to the main fault trace.

These vertical offsets can be attributed to the instability of the medial ridge itself. The fault branches form planes along which landslides occur in the interseismic period. During seismically active periods the horizontal slip is not confined to a single strand but rather is distributed onto sub-parallel faults. Complex mechanics during the earthquake may cause different fracture planes to become active or inactive depending on changing loads on the individual traces (Figs. 9a-d). These shifting forces are created when dynamic forces during an earthquake result in lateral movement along an active fault on the ridge which may sometimes lock, i.e. when the subsurface is characterized by more shearing resistant properties (Fig. 9b). Subsequently, loads are transferred to a soil mass farther upslope on the ridge that is less resistant to the applied shear forces, i.e. if the soil is slumping Fig. 9c). This will then create a new sub-parallel trending trace that accommodates the horizontal displacement (Fig. 9d). The morphology of the western slopes of the Silver Hills in the northern portions suggests the presence of multiple such strands along which we find horizontal offsets from past earthquakes, as well as soil creep, active and dormant landslides throughout the area.

4.5 Point Reyes National Seashore Headquarters

The headquarters of Point Reyes National Seashore, the former property of the Skinner Ranch, is located just south of the Silver Hills. The 1906 fault trace passes through the farmstead as a single strand (Fig. 10a). At this location, G.K. Gilbert recorded four offset measurements ranging from 4.4 to 4.9 m (14.5 ft to 16 ft) (Lawson, 1908). Figure 10b shows a reconstruction of the historic layout from Gilbert's sketch map (Lawson, 1908, p. 71) overlain on a digital orthophotograph. Gilbert discounted a 25 ft displace as it differed significant from a measurement he took nearby. In his notes he states:

> Notebook 108,Wednesday, May 9, 1906 ;
> *A cyprus tree at the Skinner place is said to have stood at a point 25' from its present position. But this is near my measure of 14.5 ft from bushes.*

Another detailed description of the coseismic slip of April 18, 1906 at the Skinner Ranch is given by David Starr Jordan (1907, pp. 20-22). He writes:

> *"The earthquake rift passed directly in front of the house, between the buildings and the road. All that stood to the westward of the crack was violently jerked to the north a distance of sixteen feet seven inches, or it may be that the east side moved an equal distance to the south."*

Studying historic documents we are able to project the measurements of both geologists to a georeferenced sketch of Gilbert (see inset Fig. 10b). Jordan measured 5.1 m of displacement of the "stone steps to the basement of the dairy" along with some 16.5 feet (5 m) offsets, two manure piles from the barn windows, and the driveway under the barn (10c and 10d). Although the offsets of cultural features measured by Jordan at the former Skinner Ranch are similar to

Gilbert's, they still generally all exceed them by a small amount and towards the NW the deviation is as high as 0.6 m (see insert in Figure 10b).

A linear depression that formed on the flank of the medial ridge southeast of the barn (Fig. 10b and 10d) (Hall 1974; 1976) collects much of the surface runoff and promotes pooling due to the disruption of the slope that prevents a downslope draining of water. Gilbert's "trench phase" (Lawson, 1908) of the fault rupture is typical for the prevailing soft, unconsolidated sediments that only support low angles of repose. Landslides are persistent throughout the area, particularly in the vicinity of the fault trace. During the earthquake, a tree south of the Skinner Ranch on a slope of the ridge toppled due to the effects of the shaking and unconsolidated subsurface sediments (Fig. 10e). The lack of pervasive pre-1906 fault geomorphic structures, such as sag ponds, drainage offsets, sub-parallel ridge, etc. at this location is noteworthy. Faulting may be distributed to other sub-parallel strands on the medial ridge that are concealed or more likely confined to the base of the slope along the Bear Valley Creek drainage. Apart from the ridge, there is no evidence for nearby Quaternary faults in the young surface deposits.

4.6 Vedanta Retreat

Approximately 1050 m southeast of the headquarters of Point Reyes National Seashore, the 1906 fault trace crosses the property of the Vedanta Religious Retreat, formerly known as Shafter Ranch (Figs. 11 a and 11b). Historic photographs and a sketch map illustrate that fault motion occurred along a single narrow trace parallel to the edge of a marsh at the base of a medial ridge (Figs. 11c and 11d). Although Gilbert did not publish the observation, he mentions in his field notes (Notebook 108, May 9, 1906) a 25 ft (7.6 m) offset estimated by Payne Shafter somewhere on his property. Otherwise, Gilbert does not provide us with an offset measurement only a clear description of the location of the fault rupture.

Subsurface excavations (Niemi and Hall 1992; Niemi, 1992; Zhang, 2005; Niemi *et al*., 2006) and aerial photo interpretations enable accurate mapping of the 1906 earthquake fault trace and other Quaternary faults (Fig. 11b). South of the Vedanta Retreat house for a distance of 425 m, the active strand of the SAF is located at the base of a ridge composed of Upper Quaternary alluvium (Grove and Niemi, 2005). The fault then steps about 8 m eastward at a wind gap between two ridges. It then traverses the slope of a steep-sided ridge where it can be identified as a sidehill bench or linear depression (Fig. 12b). The location of the fault step-over is known as Vedanta wind gap (Niemi, 1992). Paleoseismic trenches (Niemi and Hall, 1992) excavated in the wind gap revealed fault evidence of a typical left step in a right-lateral, strike-slip fault that created small thrusts striking at 300˚ and dipping at 26˚ SSE.

In his 1906 field notes archived in the Stanford University Special Collections, D.S. Jordan states:

> *A little south of Shafter Ranch a large chestnut oak tree about two feet through stood at the very edge of the crack and this has been violently shoved 16 ½ feet further south where it is pushed into the side of a hill along the margin of which the crack goes. The crack passes on the east side of this hill and there were five large fir trees growing near the crack thrown down, all of them lying WSW or nearly at right angles with the crack.*

A sketch from the Jordan notebook is shown in Figure 12d. We assume that severed roots or other debris that remained on the northwest side of the rupture trace served as a piercing point for his observation of the offset. The ridge south of the wind gap clearly shows geomorphic evidence that a slice of the ridge on the west of the SAF is displaced towards the northwest.

The ridge itself appears to have preserved the latest offsets at higher topography. An interpolated geomorphic surface of the wind gap based on RTK GPS survey data and total station measurements is shown in Figure 12b. The western side of the ridge is clearly displaced towards the northwest. We estimate the offset by matching 5 contours (at 25 cm intervals) between 31.5 m and 32.5 m elevation across the fault as they are the contours that are offset most abruptly. These elevations likely preserve the offset of the most recent earthquakes. The average displacement of the contours is 5.4 ± 3.4 m. The margin of error is relatively high because of the range of data that we used to compute the offset. However, the displacement increases at elevations below 31.5 m due to primarily heavy erosion along the northeast-facing fault scarp, cultural modifications, and cumulative fault displacement. We also determined the offset preserved by a fallen fence that we assume once extended straight across the SAF. The deflection of the fence increases towards the west and peaks at 7.4 m (Fig. 12). Because of the uncertainty in the original fence geometry it is difficult to assess the reliability of this measurement. The slip value for the fence does, however, compare favorably to a reported 25 ft (7.6 m) on the Shafter Ranch (Gilbert Notebook 108, May 9, 1906).

Our photo relocations and analyses of field notes provide useful information about the site (Fig. 12). We discovered the location of five downed Douglas fir trees that fell in the 1906 earthquake. Ancient Douglas fir trees dating to several hundred to a thousand years ago and trending perpendicular to the fault (Fig. 12c - 12e) were also found buried in the Vedanta marsh in the paleoseismic trenches of Niemi (1992). The 1906 Earthquake seemed to have a significant impact on the mostly Douglas fir trees that occupy the steep slope where the fault trace runs on the western flank of the ridge south of the wind gap. Due to high annual rainfall by the time the earthquake struck (Niemi and Hall, 1996), the fault trace that formed a linear depression on the side of the hill (sidehill bench) collected much of the surface water. This probably further weakened the gravelly alluvium that composes the escarpment along the steep-sided hill. The compromised hillslope provides a possible explanation for Jordan's description and the historic photographs of toppled fir trees after the earthquake struck.

5. Discussion

The maximum displacement of the northern SAF measured shortly after the 1906 earthquake was the 20-21 foot offset (6.1-6.4 m) (Lawson, 1908) of the Sir Francis Drake Boulevard (SFDB) road. Analyses of archival materials indicate that Gilbert himself believed these measurements may be an overestimation of the offset. Gilbert also discounted two 7.6 m (25 ft) offsets as unverifiable, especially as compared to measurements of approximately 5 m (16 - 16.5 ft) that he himself measured nearby. Gilbert knew about the importance of the effects of liquefaction and lateral spreading in possibly enhancing coseismic offset measurements (Leviton *et al.,* 2006). Brown and Wolfe (1972) also noted Gilbert's suspicions that "a reported 20-21 foot dislocation of a road at the head of Tomales Bay, often cited as the maximum slip accompanying the 1906 earthquake, was considered excessive by G.K. Gilbert."

In this paper we have compared the historical archival data with new geomorphic data collected along the 1906 SAF rupture trace in Marin County. These data help us resolve questions on coseismic slip, cumulative slip, and fault zone deformation.

At the Bear Valley Creek meander site, we analyzed the meander drainage pattern and identified potential piercing points for the investigation of recorded displacements across the SAF. Our estimates for the coseismic slip of meander loops range from 5.7 ± 0.6 m to about 7.8 ± 2.4 m. These data provide additional support to Gilbert's > 6 m offset measurement of SFDB. One tributary shows evidence of about 50 m of cumulative displacement indicating that the 1906 fault trace has been repeatedly active at the same location for several earthquake cycles. Because of lack of paleoseismic data at the site and the time interval between 1966 and the 1906 earthquake, erosion is likely to have lengthened or enhanced the channel meander leading to uncertainty in the offset measurements.

Studies have often shown that coseismic displacements measured in the field differ from geodetic models, for example the 1999 Hector Mine Hudnut *et al.*, (2002). Thatcher *et al*. (1997) calculated a 6.7 ± 0.3 m of slip for the 1906 earthquake at SFDB south of Tomales Bay and a slip of 5.6 m in the Olema Valley using a model that constrained fault locking depths at 10 km. Song *et al.* (2008) using a unified source-to-model slip and a 12-km-deep fault plane calculated the geodetic slip of the 1906 earthquake of 7.0 m south of Tomales Bay and 6.1 m for the SAF section farther south in Marin County. The geodetic slip models calculate the total offset both along faults and distributed as shear or ductile deformation across the fault zone. Nonetheless, coseismic displacements both measured by G.K. Gilbert and our geomorphic data are in general agreement with the modeled geodetic values.

Offsets that occur as a result of an earthquake are often not constrained to a single plane of motion. Documentations of surface fault rupture crossing fence lines in Lawson (1908) are indicative of the complex faulting on multiple active strands across the strike-slip fault zone. The pattern of distributed shear known as fault drag can be observed in small-scale models (Lazarte and Bray, 1996), and is well documented for recent earthquakes, such as the 1999 Turkey earthquakes and the 2002 Denali earthquake (Rockwell *et al.*, 2001; Eberhart-Phillips *et al.*, 2003). Prentice and Ponti (1997) studying the 1906 deformation of Wright tunnel in the Santa Cruz Mountains found that 60-85% of the displacement was confined to a single fault plane of the SAF. Bray and Kelson (2006), who also studied the 1906 fault rupture and its effects on the built environment, show that simple shear is distributed as far away as a few hundred meters from the immediate surface rupture trace. However, the slip of the SAF south of Tomales Bay appear to be in some locations confined to a single, narrow trace that accommodates most of the 1906 offset, rather than forming a widely distributed zone with spatial variations.

The pattern of coseismic offset and deformation along an earthquake rupture appears to depend strongly on the properties of the subsurface material. This is particularly evident at the Silver Hills site southeast of SFDB road and Bear Valley Creek meanders, where the 1906 fault trace runs along the edge of a ridge composed of Upper Pleistocene sediment (Hall and Hughes, 1980). Borchardt (2010) reports that mature shear zones with more than 30 events are confined to a narrow zone while young sediment are characterized by wider fault zones. Our data of the SAF zone in Marin County indicate that the rupture trace in some locations is geologically young.

The variation of coseismic offset along strike of a fault rupture in an earthquake has been widely documented. Analyses of well-preserved cultural offsets at the former Skinner Ranch (1.5 km southeast of the Silver Hills) shows that Gilbert's measurements deviate by as much as 0.5 m along a profile of 180 m and that the observations of the same site can differ up to 0.7 m between distinguished geologists Gilbert and Jordan. We can infer that all coseismic measurements include some inaccuracies and are probably somewhat subjective. The historic measurement we found at the Vedanta site compares well with the measurements at the former Skinner Ranch ~ 5 m (16 -16.5 ft) and our estimate of the deflection in the ridge (4.0 ± 2.1) south of the wind gap. Nonetheless, a second measurement we obtained from a nearby fence that crossed the 1906 fault trace and was in part preserved, shows as much as 7.4 m of deflection from its straight-line course. This value is close to the disregarded 7.6 m offset suggesting that higher offsets in this area were possible also keeping in mind that offset measurements can vary greatly within short distances. We deduce that the high offsets reported from the meander loops of the creek south of SFDB in conjunction with the concepts of distributed shear and geodetically modeled slip estimates, give strong support for a local maximum of observed coseismic slip of the 1906 earthquake > than 7m.

6. Conclusion

In our study we evaluate published and unpublished documents with the goal of identifying coseismic surface deformation and improving earlier estimates of displacements south of Tomales Bay in Olema Valley. Whereas previous studies quantify coseismic displacements ranging from 4.4 m to 6.4 m at Point Reyes National Seashore, we found evidence suggesting that slip exceeded 7 m in places. This potential seems particularly evident in the northernmost extent of Olema Valley where the 1906 fault motion is confined to a narrow trace with low amounts of distributed off-fault shear. Our data suggest that historical accounts of 25 ft (7.6 m) of coseismic offset in the 1906 earthquake should not be discounted. Our slip estimate also agrees well with geodetically modeled slip values.

Although, the 1906 trace is still clearly visible in much of our study area, large tracts of land that were pasture in 1906 have become overgrown and has obscured the fault trace. As part of our study, we propose new and refined locations of Quaternary faults beyond the trace that was active during the 1906 earthquake. In areas affected by Quaternary faulting, we identify tectonic geomorphic processes that determine the morphologic response of the landforms during events of seismically active and inactive periods. The surface deformations caused by the earthquake rupture vary throughout the investigated area. Alluvial ridges are characterized by the formation of subparallel trending faults that create sidehill benches and trench-like features (Vedanta) and more widely subparallel distributed slip when mass wasting processes concur with seismic loading (Silver Hills). During periods of seismic inactivity, former rupture traces can be obscured, degraded by erosion and mass wasting and subsequently replaced by landslide scarps. Our results can help to identify crucial sites where similar deformations along the SAF are probable in the future and that further morphotectonic and paleoseismic investigations are necessary to better constrain measureable coseismic slip.

7. Acknowledgements:
This research was supported by a grant from the U.S. Geological Survey (USGS) NEHRP award number 06HQGR0014 to Niemi. The views and conclusions contained in this document are those of the authors and should not be interpreted as necessarily representing the official policies, either expressed or implied, of the U.S. Government. The Vedanta Society of Northern California generously granted access to the Vedanta Retreat in Olema. We thank Superintendent Don Neubacher, Ben Becker, Carola DeRoy, Sarah Allen and other National Park personnel for permission and assistance in conducting fieldwork in the Point Reyes National Seashore. This project was greatly facilitated by N. Timothy Hall who provided invaluable historic materials and Carol Prentice (USGS) who provided us a copy of the D.S. Jordan notebook. We thank Francisco (Paco) Gomez from the University of Missouri - Columbia for providing RTK GPS equipment that was crucial to this study.

8. Bibliography of all publications resulting from the work performed under the award:

1. Daehne, A., and Niemi, T.M., submitted 2012, Coseismic deformation and new slip estimates of the 1906 San Francisco Earthquake rupture on the San Andreas fault in Marin County, California: *Tectonophysics.*

2. Daehne, A., 2007, Investigation of Quaternary Fault Deformation and Coseismic Slip of the 1906 Earthquake in Marin County, California: M.S. Thesis, Department of Geosciences, University of Missouri-Kansas City, 249p.

3. Daehne, A., and Niemi, T.M., 2007, Investigation of Quaternary fault deformation and coseismic slip of the 1906 earthquake in Marin County using the Lawson report and unpublished documents: Annual Meeting, *Geological Society of America,* Denver, CO, Oct. 27-31, 2007.

4. Niemi, T.M., Hall, N.T., and Daehne, A., 2006, The 1906 earthquake rupture trace of the San Andreas fault north of San Francisco, in C.S. Prentice, J.G. Scotchmoor, E.M. Moores, and J.P. Kiland (eds.), *1906 San Francisco Earthquake Centennial Field Guides: Field Trips Associated with the 100th Anniversary Conference, April 18-23, 2006, San Francisco, CA*: Geological Society of America, p. 157-176.

5. Daehne, A., and Niemi, T.M., 2006, Using the Lawson Report and other historical documents to investigate fault morphology and coseismic slip of the 1906 earthquake in Marin County: Annual Meeting, *Seismological Society of America,* SF, CA, April 18-22, 2006, *Seismological Research Letters*, v. 77 (2), p. 249.

9. References

Boatwright, J., Bundock H.K., 2005. Modified Mercalli Intensity Maps for the 1906 San Francisco Earthquake Plotted in ShakeMap Format Version 1.0., U.S. Geol. Surv. Open-File Report 2005-1135.

Boatwright, J., Bundock, H.K., 2008. The distribution of modified Mercalli intensity in the 18 April 1906 San Francisco earthquake, Bull. Seismol. Soc. Am. 98**,** no. 2, 890-900.

Borchardt, G., 2010. Establishing appropriate setback widths for active fault: Environ. & Eng. Geosc, 26, no. 1, 47-53.

Bray, J.D., Kelson K.I., 2006. Observations of surface fault rupture from the 1906 earthquake in the context of current practice. Earthquake Spectra 22, no. S2, S69-S89.

Brown R. D., Wolfe, E. W., 1972. Map showing recently active breaks along the San Andreas fault between Point Delgada and Bolinas Bay, California, U.S. Geol. Surv. Misc. Geol. Invest. Map I-692, scale 1:24,000.

Bryant, W. A. (compiler), 2005. Digital database of Quaternary and younger faults from the fault activity map of California, version 2.0, Calif. Div. Mines. Prel. Geol. Map, http://www.consrv.ca.gov/CGS/information/publications/Pages/QuaternaryFaults_ver2.aspx (last accessed July 2012).

California Geological Survey (CGS), 2001. GIS files of the official Alquist-Priolo earthquake fault zones, central coastal region, Calif. Geol. Surv. CD 2001-04.

Clark, J.C., Brabb, E.E., 1997. Geology of the Point Reyes National Seashore and Vicinity, CA: A digital database, U.S. Geol. Surv. Open-File Rept. 97-456.

Daehne, A., 2007. Investigations of Quaternary fault deformation and coseismic slip of the 1906 earthquake in Marin County, California. Master's Thesis, University of Missouri – Kansas City, Kansas City, Missouri, 249 pp.

Eberhart-Phillips, D., Haeussler, P. J., Freymueller, J. T., , Frankel, A. D., Rubin, C. M., Craw, P., Ratchkovski, N. A., Anderson, G., Carver, G. A., Crone, A. J., Dawson, T. E., Fletcher, H., Hansen, R., Harp, E. L., Harris, R. A., Hill, D. P., Hreinsdottir, S., Jibson, R. W., Jones, L. M., Kayen, R. D. Keefer, K., Larsen, C. F., Moran, S. C., Personius, S. F., Plafker, G., Sherrod, B. Sieh, K., Sitar, N., Wallace,W. K., 2003. The 2002 Denali fault earthquake, Alaska: a large magnitude, slip-partitioned event. Science 300, 1113-1118.

Federal Geographic Data Committee (FGDC), 1998. Geospatial Positioning Accuracy Standards Part 3: National Standard for Spatial Data Accuracy, FGDC-STD-007.3-1998.

Galloway, A. J., 1977. Geology of the Point Reyes Peninsula, Marin County, California, Cal. Div. Mines and Geol**.** Bull. 202, 72 pp., plus 1:48,000-scale plate.

Gilbert, G. K., 1907. The earthquake as a natural phenomenon. In: The San Francisco Earthquake and Fire of April 18, 1906, and their Effects on Structures and Structural Materials. U.S. Geological Survey Bull. 324, 1-13.

Grove, K., Colson, K., Binkin, M., Dull, R., Garrison, C., 1995. Stratigraphy and structure of the Late Pleistocene Olema Creek Formation, San Andreas fault zone north of San Francisco, California. In Sangines, E., Andersen, D., Buising, A. (Eds.), in: Recent Geologic Studies in the San Francisco Bay Area, Society for Sedimentary Geology (SEPM) Pacific Section Book 76, pp. 55-77.

Grove, K., Niemi T.M., 2005. Late Quaternary deformation and slip rates in the northern San Andreas fault zone at Olema Valley, Marin County, California, Tectonophysics, 401, No. 3-4, 231-250.

Grove, K., Sklar, L.S., Schere, A.M., Lee, G. Davis, J. 2010. Accelerating and spatially-varying crustal uplift and its geomorphic expression, San Andreas Fault zone north of San Francisco. Tectonophysics, 495, 256-268.

Hall, N.T., 1974. The Earthquake Trail at Point Reyes National Seashore, California Geology 27**,** no. 4, 87-89.

Hall, N.T., 1976. Earthquake Trail revisited: California Geology 29**,** no. 9, 206-207.

Hall, N.T., Hughes, D.A., 1980. Quaternary geology of the San Andreas fault zone at Point Reyes National Seashore, Marin County, California, in: Streitz, R., Sherburne, R. (Eds.), Studies of the San Andreas Fault Zone in Northern California, Calif. Div. Mines and Geol. Spec. 140, pp. 71– 87.

Hall, N.T., Hayand, E.A., Cotton, W.R., 1986. Investigation of the San Andreas fault and the 1906 earthquake, Marin County, California: National Earthquake Hazards Reduction Program Final Technical Report, Contract #14-08-0001-21242, 3 maps, scale 1:1200.

Hudnut, K. W., King, N. E., Galetzka, J. E., Stark, K. F., Behr, J. A., Aspiotes, S. van Wyk, A., Moffitt, R. Dockter, S., Wyatt, F., 2002. Continuous GPS observations of postseismic deformation following the 16 October 1999 Hector Mine, California, earthquake (M_w 7.1), Bull. Seism. Soc. Am. 92**,** 1403–1422.

Johnston, K., Ver Hoef, J., Krivoruchko, K., Lucas, N., 200. Using ArcGIS Geostatistical Analyst, GIS by ESRI, 300 p.

Jordan, D.S. (Ed.), 1907. The California Earthquake of 1906. A.M. Robertson, San Francisco, 360 p.

Lawson, A. (Ed.), 1908. The California Earthquake of April 18, 1906; Report of the State Earthquake Investigation Commission. Carnegie Institute, Washington, Publ. 87. (451 pp., Reprinted 1969).

Lazarte, C.A., Bray, J.D., 1996. A study of strike-slip faulting using small-scale models, *Geotech. Test. Journ.*, American Society for Testing and Materials, 19 (2), 118-129.

Leviton, A. E., Aldrich, M. L., Elsbernd, K., 2006.The California Academy of Sciences, Grove Karl Gilbert, and photographs of the 1906 Earthquake, mostly from the archives of the Academy, Proceedings of the California Academy of Sciences, ser. 4 57, 1, 1–34.

Livingston, D.S., 1993. Ranching on the Point Reyes Peninsula : a History of the Dairy and Beef Ranches within Point Reyes National Seashore, 1834-1992, Point Reyes Station, CA : National Park Service. 544p.

Livingston, D.S.,1995. A Good Life: Dairy Farming in the Olema Valley: A History of the Dairy and Beef Ranches of the Olema Valley and Lagunitas Canyon, Golden Gate National Recreation Area and Point Reyes National Seashore, Marin County, California, National Park Service, Dept. of the Interior, 491p.

Niemi, T.M., 1992. Late Holocene slip rate, prehistoric earthquakes, and Quaternary neotectonics of the Northern San Andreas fault, Marin County, California. Ph.D. Dissertation, Stanford University, 199p.

Niemi, T.M., Hall, N.T. (1992). Late Holocene slip rate and recurrence of great earthquakes on the San Andreas fault in northern California, Geology, 20, 195-198.

Niemi, T.M., Hall, N.T., 1996. Historical changes in the tidal marsh of Tomales Bay and Olema Creek, Marin County, California, Journ. of Coastal Res. 12(1), 90-102.

Niemi, T.M., Hall, N.T., Daehne, A., 2006. The 1906 earthquake rupture trace of the San Andreas fault north of San Francisco, in: C.S. Prentice, J.G. Scotchmoor, E.M. Moores, and J.P. Kiland (eds.), 1906 San Francisco Earthquake Centennial Field Guides: Field Trips Associated with the 100th Anniversary Conference, April 18-23, 2006, San Francisco, CA. Geological Society of America, Centennial Field Guide 7, pp. 157-176.

Prentice, C.S., Ponti, D.J., 1997. Coseismic deformation of the Wrights tunnel during the 1906 San Francisco earthquake: A key to understanding 1906 fault slip and 1989 surface ruptures in the southern Santa Cruz Mountains, California, J. Geophys. Res. 102 (B1), 635-648.

Rockwell, T.K., Lindwall, S., Dawson, T., Langridge, R., Lettis, W.R., 2001. Lateral offsets on surveyed cultural features resulting from the 1999 Izmit and Düzce earthquakes, Turkey, Bull. Geol. Soc. Am. 91 (1), 79-94.

Schumm, S., Dumont, J. F., Holbrook, J. M., 2000. *Active Tectonics and Alluvial Rivers*, Cambridge University Press, Cambridge, 276p.

Song, S.G., Beroza, G.C., Segall, P., 2008. A unified source model for the 1906 San Francisco earthquake. Bull. Geol. Soc. Am. 98, no. 2, 823-831.

Thatcher, W., Marshall, G., Lisowski, M., 1997. Resolution of fault slip along the 470-km-long rupture of the great 1906 San Francisco earthquake and its implications, J. Geophy. Res. 102, B3, 5353 –5367.

Tchalenko J. S., 1970. Similarities between shear zones of different magnitudes, Bull. Geol. Soc. Am. 81, 1625-1640.

Wallace, R.E., 1968. Notes on stream channels offset by the San Andreas Fault, southern Coast Ranges - California, Stanford Univ. Pub. Geol. Sci. 11, 6-21.

Wallace, R.E., 1980. G. K. Gilbert's studies of faults, scarps, and earthquakes, in: The scientific ideas of G.K. Gilbert, E.L Yochelson (Ed), Geol. Soc. Am. Spec. Pap. 183, pp. 35-44.

Wilcox R. E., Harding T. P., Seely, D. R., 1973. Basic wrench tectonics, Am. Assoc. Petrol. Geol. 57, 74-96.

Working Group on California Earthquake Probabilities (WGCEP), 2003. Earthquake probabilities in the San Francisco Bay region: 2002 to 2031—a summary of findings, U.S. Geol. Surv. Open-File Rept. 03- 214.

Zhang, H., 2005. Paleoseismic studies of the northern San Andreas fault at Vedanta Marsh site, Olema, California, Ph.D. Thesis, University of Missouri-Kansas City, Kansas City, 334 p.

Table 1: Data and Resources

- Some historical photographs by J.C. Branner were used for the Vedanta site. The photos were acquired in the early 1990s from the geology department at Stanford University. An inquiry about the whereabouts of the collection today remained unsuccessful.
- ArcGIS Desktop version 8.2 and 9.2 ArcView® and Spatial Analyst® from Environmental Research Institute (ESRI) were used.
- For processing of GPS survey data Trimble Geomatics Office™ software version 1.5 was used.
- Digital Orthophoto Quarter Quadrangles (DOQQ), GeoTiff format, State plane Coordinate System, California Zone 3, FIPS 403, North American Datum of 1983. Data can be obtained from the Marin General Services Authority at http://mmgis.marinmap.org/OrthoGrid/viewer.htm (last accessed July 2009).
- USGS 24,000-scale digital elevation models (DEM) available from 1/3 ARC Second National Elevation Dataset (NED), ArcGrid format, approximately 10 m resolution at http://seamless.usgs.gov/website/seamless/viewer.htm (last accessed July 2009).
- USGS 24,000-scale Digital Line Graphs (DLG), available online at http://dds.cr.usgs.gov/pub/data/DLG/LARGE_SCALE/P/point_reyes_ne_CA/ (last accessed May 2010)
- A map produced by the U.S. Coastal Survey map in 1862 was directly acquired from the library of Point Reyes National Seashore.
- Historic 7.5-minute and 15-minute Topographic maps are downloadable from UC Berkeley library as scanned un-georeferenced digital raster graphics (DRG) in sid format at http://sunsite.berkeley.edu/histopo/ (last accessed July 2009).
- DOQQs from the 1990's were obtained directly from the GIS department of Point Reyes National Seashore. No metadata were available for these orthophotos.
- Gilbert's field notes are available at USGS library in Denver. A copy was obtained in the early 1990's.
- LiDAR data in the Olema valley were acquired as part of the NoCAL project. Data and DEMs are available online for download at the Open Topography Portal: http://www.opentopography.org/ (Last accessed May 2010).

Electronic Supplement

The electronic supplement maybe accessed online (no later than 4 Sep, 2010) using the following URL:
http://cdm.unimore.it/dep/$%ESupp.zip

Table 2: Offsets of the 1906 Earthquake between Bolinas Lagoon and Tomales Bay

Site No.	Location Name & Coordinates*	Offset	Feature	Fault character	Reference**
1	Sir Francis Drake Blvd N4212804 E516 398	20-21 ft (6.1-6.4 m)	Road	Fault trace 50-60 ft wide (15-18 m)	p. viii, 21, 53, 148 (21 feet); p. 71, 114, 148 (20 feet)
2	Skinner Ranch N 4210617 E 517772	15.5 ft (4.7 m)	Fence S of barn	Single narrow zone	p. 70-71
		16 ft (4.9 m)	SE corner of cow barn	Single narrow zone	p. 70-71
		15 ft (4.6 m)	Path in garden	Single narrow zone	p. 70-71
		15.75 ft (4.8 m)	Path in garden	Single narrow zone	Plate 38 D
		14.5 ft (4.4 m)	Row of raspberry bushes	Single narrow zone	p. 70-71
		25 ft (7.4 m)	Cypress tree offset	No description	G.K. Gilbert's field notes
		16 ft 7 in (5.1)	Row of cypress, eucalyptus, path, raspberry; Stone steps to dairy basement	Single narrow zone	Jordan (1907)
		16.5 ft (5 m)	Barn SE corner, driveway under barn; 2 manure piles from barn window	Single narrow zone	Jordan (1907)
3	Shafter Ranch N 4209312 E 518585	16.5 ft (5 m)	Gateway leading to road at side of barn	No description	David Starr Jordan (Stanford Archives)
		16.5 ft (5 m)	Large chestnut oak tree	Sketch shows one strand	David Starr Jordan (Stanford Archives)
		25 ft (7.4 m)	"similar offsetting" possibly tree or fence	"not verified"	G.K. Gilbert's field notes
4	Strain Ranch N 4199802 E 525365	15 ft (4.6 m)	Bent fence	2 strands, diffused shear	p. 70
		11 ft (3.4 m)	Offset and bent fence	1 strand & diffused shear	p. 70
		13.5 ft (4.1 m)	Row of eucalyptus	*En echelon* fault trace	p. 70
5	*North of Bolinas* Southworth Ranch	>12 ft (>3.7 m)	Fence	Diffuse zone	p. 70

*UTM ZONE 10, NAD83
**Page numbers from Lawson (1908).

Table 3. Compilation of sources for historic earthquake images.

Source	Photographer	Location*	Resolution in dots per inch (dpi) and type of image
U.S. Geological Survey Photographic Library	Grove Karl Gilbert, 1906 and 1907	http://libraryphoto.cr.usgs.gov/ (last accessed July 2009) (publicly accessible)	• 100 as thumbnail-resolution GIF file • 700 as medium-resolution JPG file • 1400 as high-resolution JPG file • 1600+ as full-resolution JPG file
The Bancroft Library - The 1906 San Francisco Earthquake and Fire Digital Collection	Harry Oscar Wood and others (unknown), 1906	http://bancroft.berkeley.edu/ collections/earthquakeandfire/index2.html (last accessed July 2009) (publicly accessible)	72 as JPG file
James B. Macelwane Manuscript Collection at PIUS XII MEMORIAL LIBRARY (Saint Louis University),	James Bernard Macelwane 1923 and 1928	James B. Macelwane Manuscript Collection at PIUS XII MEMORIAL LIBRARY (Saint Louis University), 3650 Lindell Blvd., St. Louis, MO 63108 (for access please contact the owner directly)	300 as TIFF or JPG file

*In all cases the images were scanned and processed by the supplier.

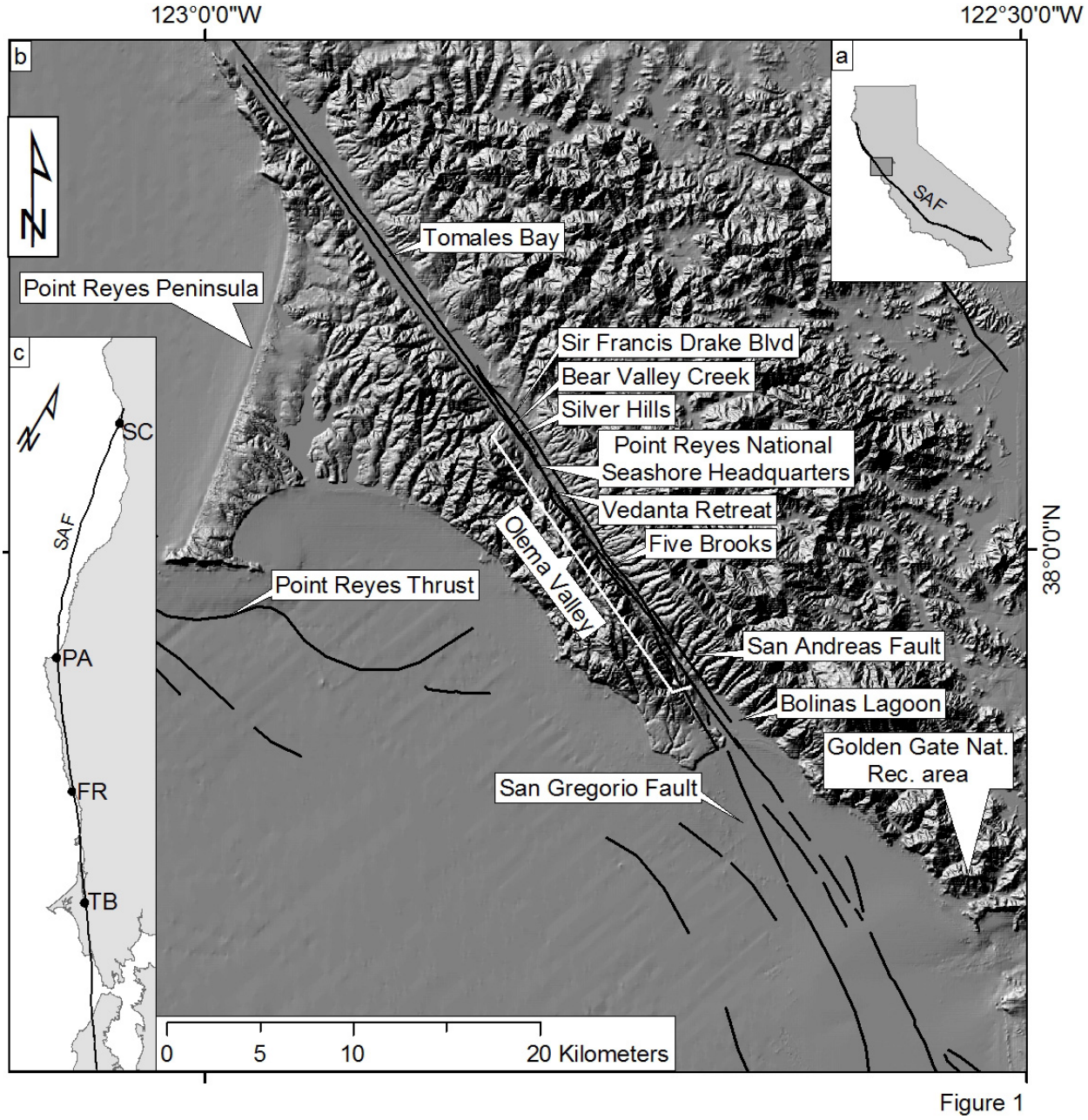

Fig. 1: a) San Andreas fault zone in California. b) Active faults in the Point Reyes area and other active faults in the San Francisco Bay. Study sites are marked. c)The 1906 fault rupture north of San Francisco (SAF). Major paleoseimic locations along the rupture trace are marked: Shelter Cove (SC), Point Arena (PA), Fort Ross (FR), Tomales Bay (TB).

Fig. 2: a) Aerial photograph of Tomales Bay with fault locations from various sources. The map shows photo points where historic sites and offsets of the 1906 earthquake were relocated by geologic field reconnaissance and remote sensing. B) A sketch map constructed by Grove Karl Gilbert that shows the 1906 fault trace crossing the head of Tomales Bay (Figure 24 on page 222 in Lawson,1908). C) "Head of Tomales Bay and delta of Papermill Creek, looking north from spur of Mount Whittenberg. Marin County, California. 1907." (From USGS Photolibrary Archive. Grove Karl Gilbert, 1907).

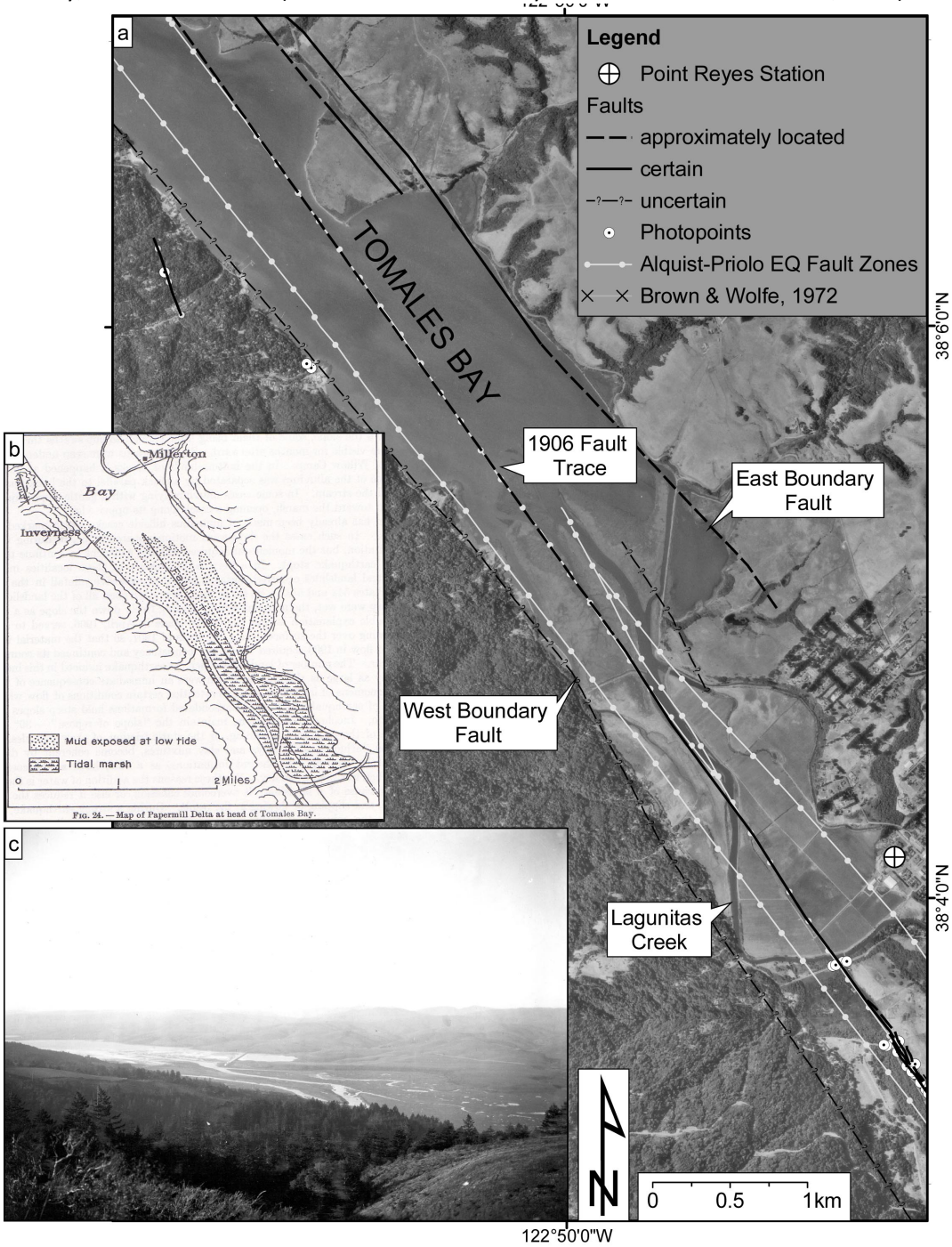

Figure 2

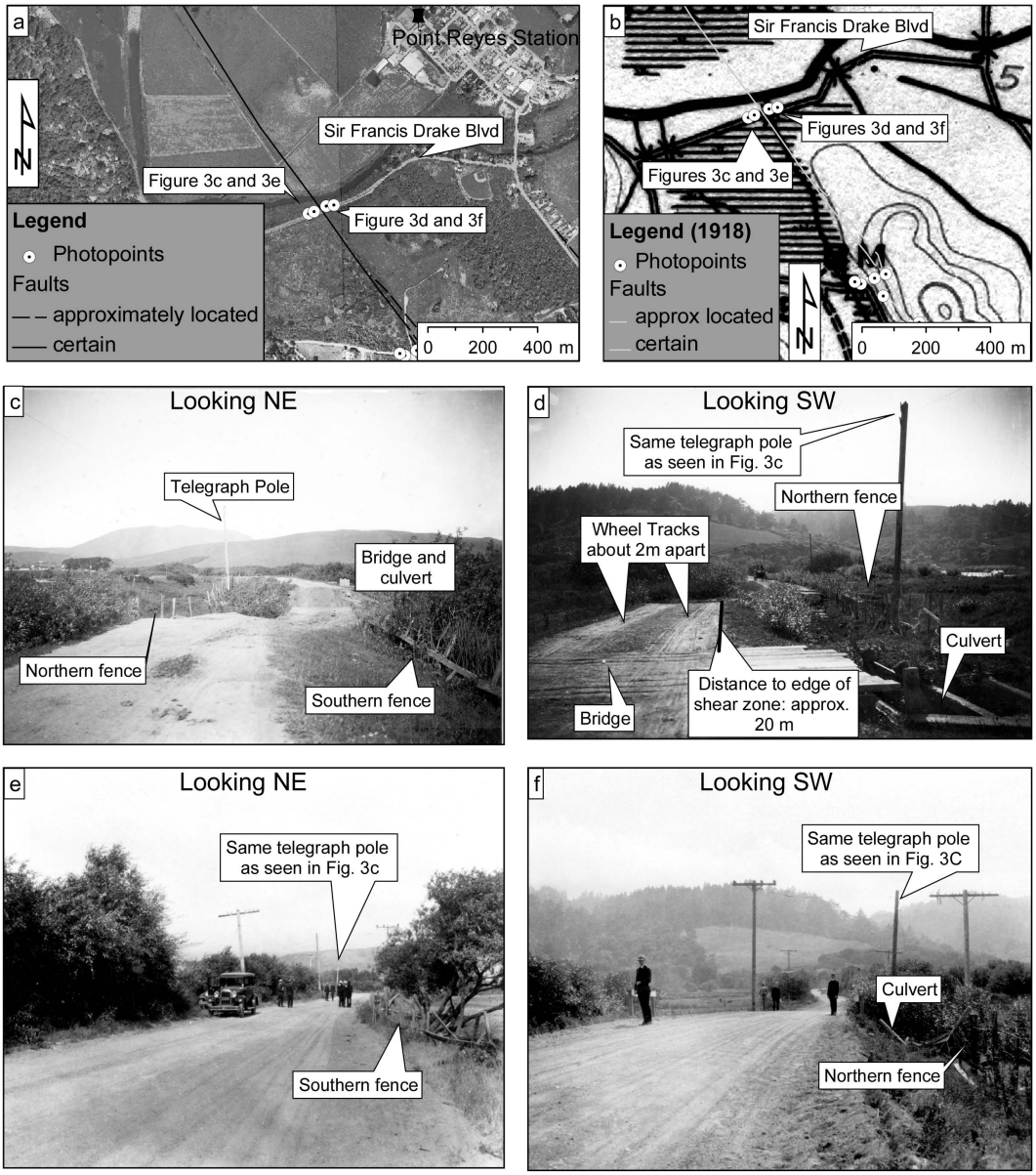

Figure 3

Fig. 3: The 1906 road offset of Sir Francis Drake Boulevard. a) Location map of the road west of the town of Point Reyes Station. b) A portion of the 1:62,500-scale topographic map from 1918 showing Sir Francis Drake Boulevard south of Lagunitas Creek. c) "Earthquake April 18, 1906. Road crossing near Point Reyes Station offset 20 feet. View is northeast. April 28, 1906." (From U.S. Geological Survey Photo Library Archives. Grove Karl Gilbert, 1906). d) The caption to this photo states: "San Francisco, California, Earthquake April 18, 1906. Effects along the fault trace. The fault trace or fracture accompanying the earthquake is inconspicuous, although the horizontal displacement is considerable. Road crossing the fault track near Point Reyes Station. View is southwest. The offset is 20 feet. The shear zone is 60 feet wide here and traverses a swamp. The road was raised above the swamp by an embankment. Between the limits of the shear zone, this embankment settled to the general level of the swamp, about 3.5 feet. April 28, 1906. Plate 1-A, U.S. Geological Survey Bulletin 324." View to the southwest. (From U.S. Geological Survey Photo Library Archives. Grove Karl Gilbert, 1906 San Francisco, California, Earthquake April 18, 1906). e) " California - Inverness Road offset 21 feet in 1906, looking west. (8/7/1928)" (Original captions from the back of photograph). The same road offset view as seen in 3c. View toward the east. Note the telegraph pole from 1906 image and the new electric lines. (James B. Macelwane Manuscript Collection at PIUS XII MEMORIAL LIBRARY (Saint Louis University), 1928). f) "Looking northwest up San Andreas Rift from above water tank on the Inverness Road northwest of Olema. 8/7/1928" The same road offset view as seen in 3d. View toward the west. (James B. Macelwane Manuscript Collection at PIUS XII MEMORIAL LIBRARY (Saint Louis University), 1928).

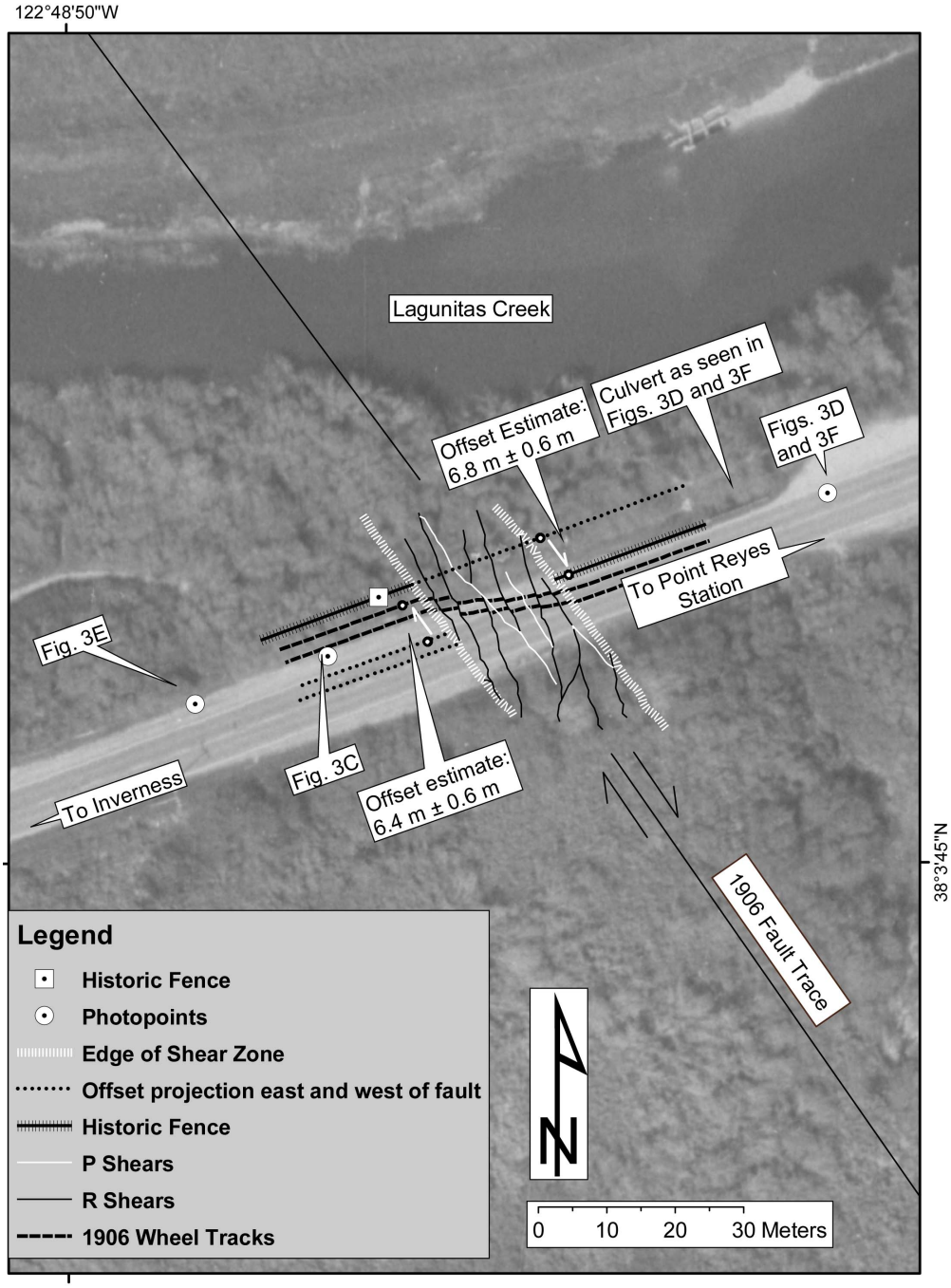

Figure 4

Fig. 4: Structural interpretation of G.K. Gilbert's road offset map published in the Lawson Report (1908) overlain onto a recent aerial photograph. Gilbert described an up to 18-m-wide zone of subsidence in the fault zone and about 6 m of horizontal offset. The wheel tracks from buggies that traveled on the Sir Francis Drake Boulevard as seen from the historic photographs and sketch (Fig. 5c) have been georeferenced in this image. An extant 1906-era fence post which we speculate to be part of the position of the historic fence flanking the old road. Projecting this fence to the northeast suggests about 5 m offset across the fault. We also mark the locations where the historical photographs (Fig. 3) were taken.

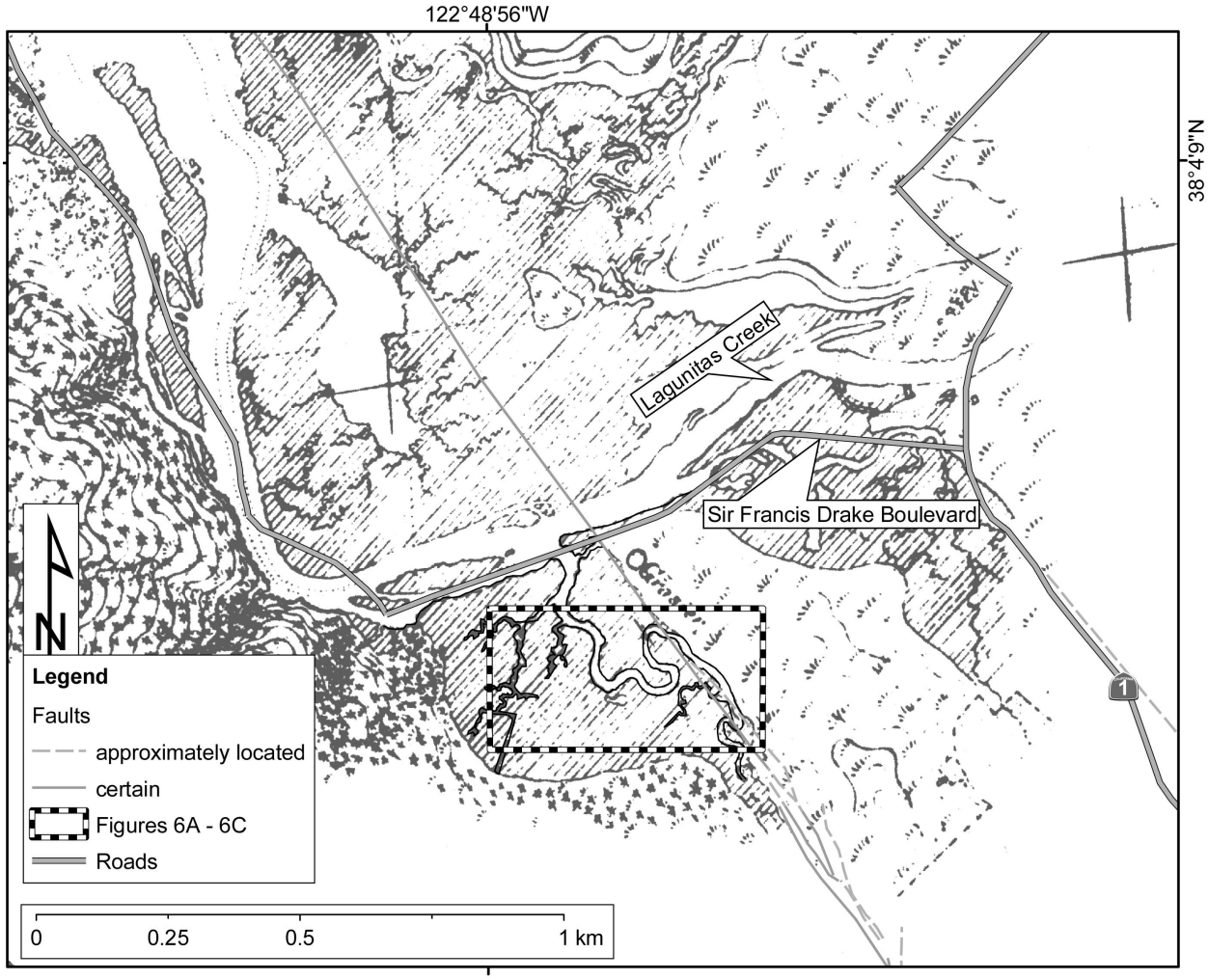

Figure 5

Fig. 5: The 1862 United States Coast Survey map showing the head of Tomales Bay and the pre-1906 earthquake meander loop patterns of the Bear Valley Creek marsh. The map further shows the location of the 1906 fault trace and other quaternary faults. The locations of today's Sir Francis Drake Boulevard and Highway 1 are overlain on the historic map.

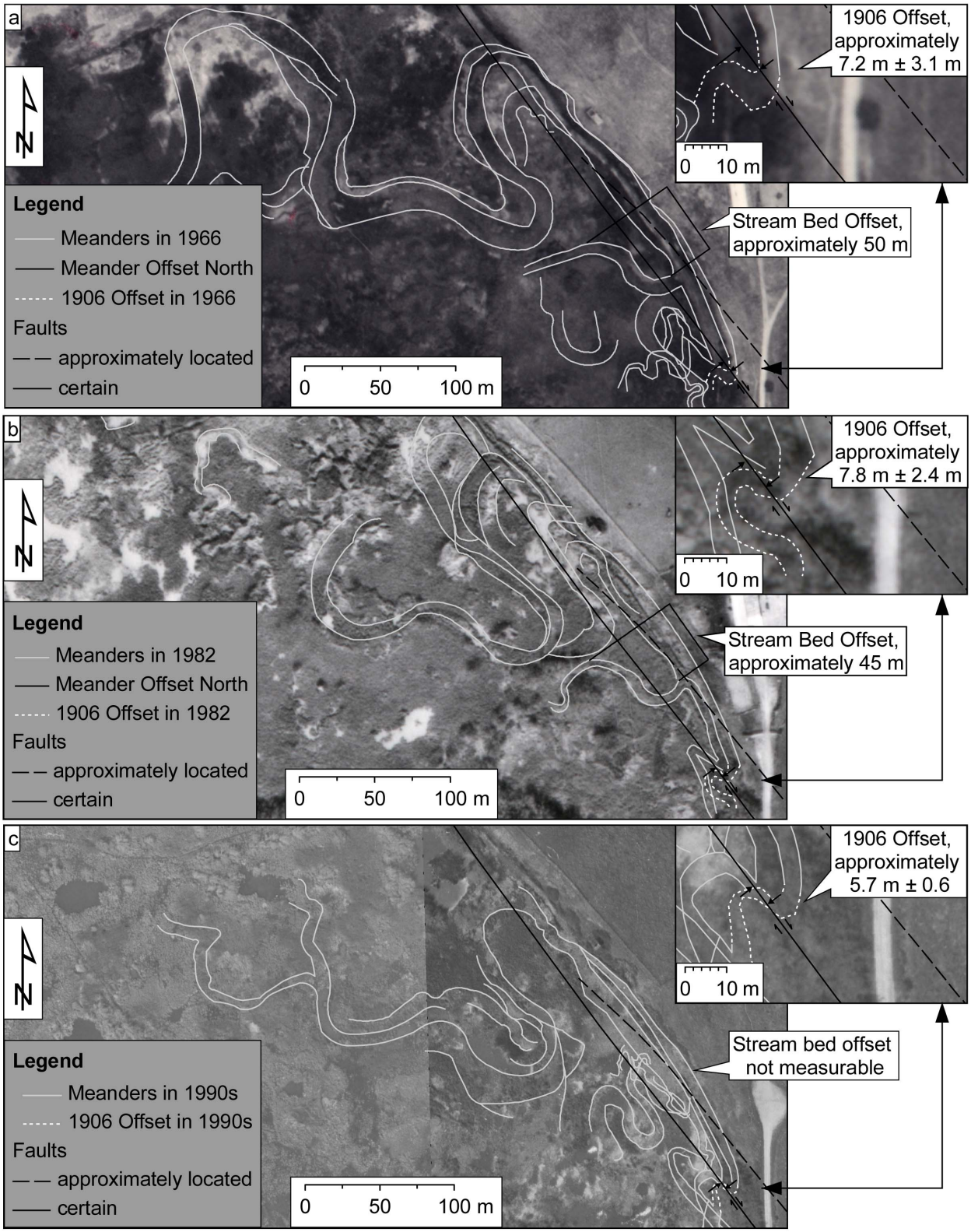

Figure 6

Fig. 6: Comparison of offset stream meanders in the Bear Valley Creek drainage. Interpretations from aerial imagery a) 1966, b) 1982, and c) mid-1990's. See text for explanation.

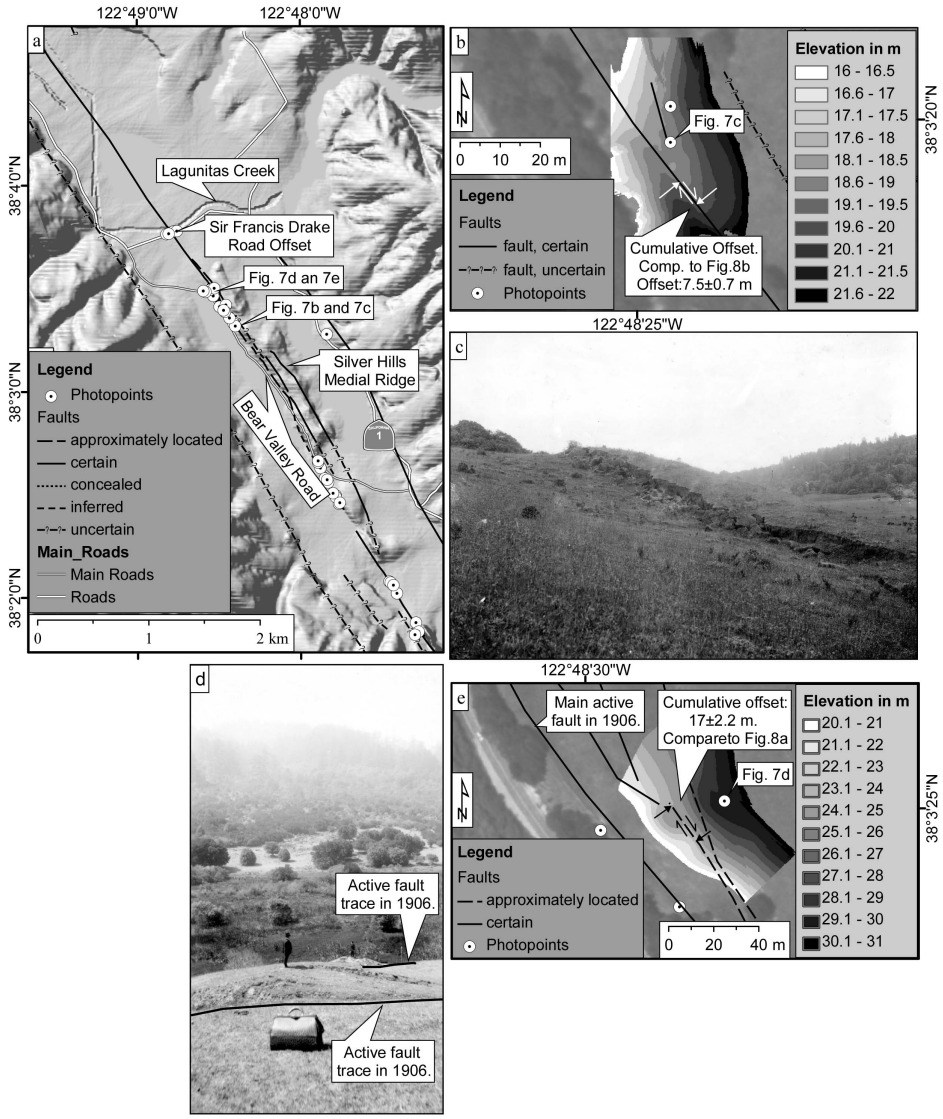

Figure 7

Fig. 7: Tectonic geomorphology of Silver Hills. a) DEM with the location of fault traces, historical photo relocation points, and areas of detailed topographic mapping. b) Bear Valley Road. This image shows the area photographed in figure 7e. A kriged surface interpolation was created from elevation data collected during a real-time kinematic GPS survey. The map shows a ridge spur offset across several fault strands. c) Digital topographic map of the 1906 fault trace photographed by G.K. Gilbert shown in Figure 7d. The elevation surface was created by kriging interpolation of elevation data collected during a real-time kinematic GPS survey. The offset along the western fault trace was determined matching contours of similar elevation across the fault. Assuming only simple shear, the horizontal slip at this location is about 7.5 ± 0.7m (compare to Figures 8a and 8b). d) Historical photograph showing an uphill facing scarp along the 1906 rupture trace on Silver Hill viewed toward the southwest. The original caption reads: “San Francisco, California, Earthquake April 18, 1906. Main fault between Olema and Point Reyes Station. View is southeast. The apparent upthrow is chiefly due to the combination of horizontal throw with slope. The knob touched by the fault is a topographic feature created by earlier movements of the same sort. 1906.” (Photo by G.K. Gilbert, 2843. From U.S. Geological Survey Photo library archive) e) Historical photograph of the offset ridge knob as viewed west across the fault strands taken in 1928 by James B. Macelwane (Courtesy of Pius XII Memorial Library at Saint Louis University). Original caption reads: "Secondary cracks, slumps, and offset ridge in pasture southwest of Point Reyes Station". The satchel and man are aligned on the uphill portion of the ridge spur, while the man in the distance is on the northwest-translated, downhill portion of the ridge.

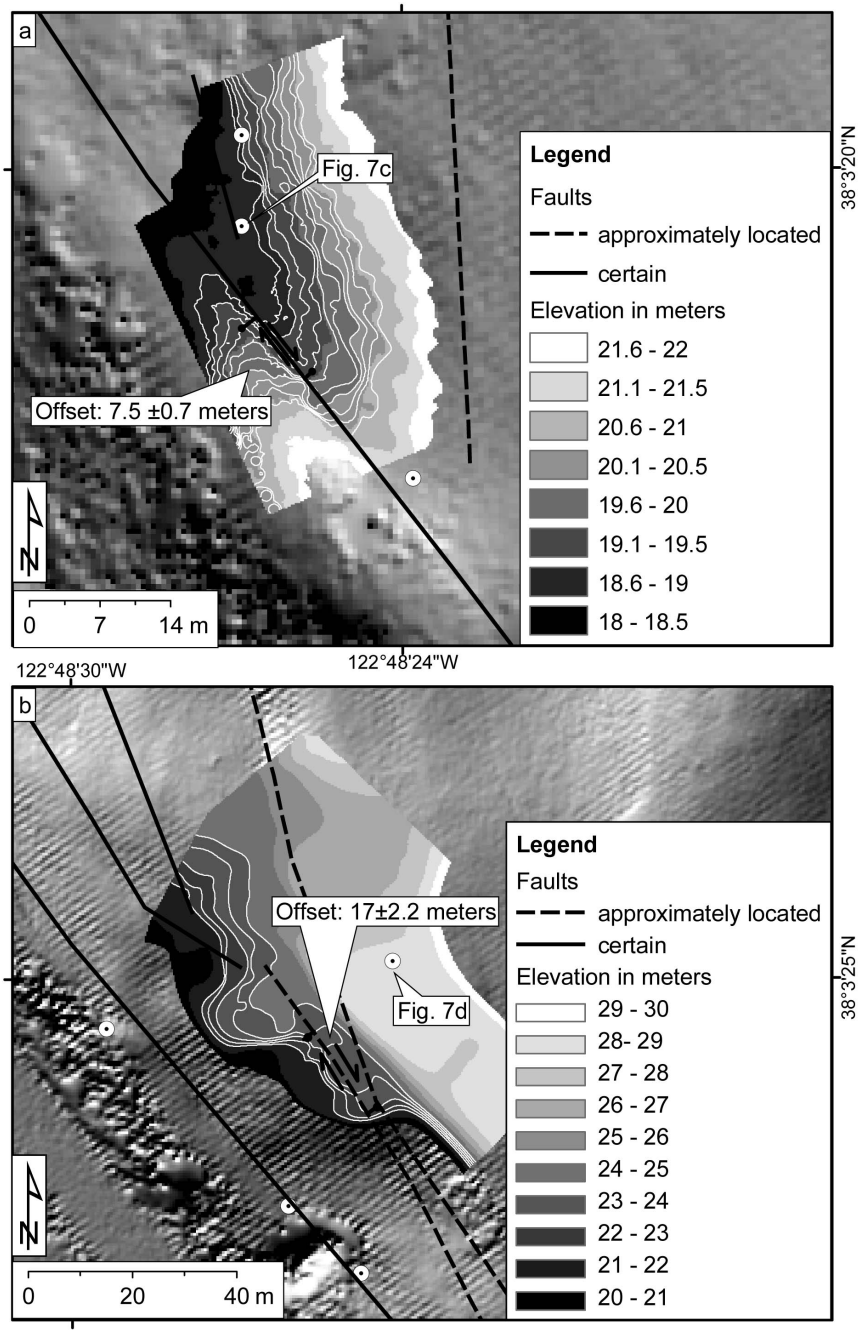

Figure 8

Fig. 8: Model of two offsets of the ridge at Silver Hills using an inverse-distance-weighting-surface interpolation a) This image shows the offset ridge spur shown in Fig. 7b and 7e. Multiple subparallel-trending fault strands are mapped from interpretation of air photo and field investigations. Comparison of the contoured topographic surface and estimates of offsets of individual contours across the fault traces yielded similar offset measurements of 17 ± 2.2m compared to those determined kriging interpolation. b) Model of the offset ridge slice shown in Fig. 7c and 7d. The cumulative offset appears to be 7.5 ± 0.7m determined by matching the deflected contours east and west of the fault.

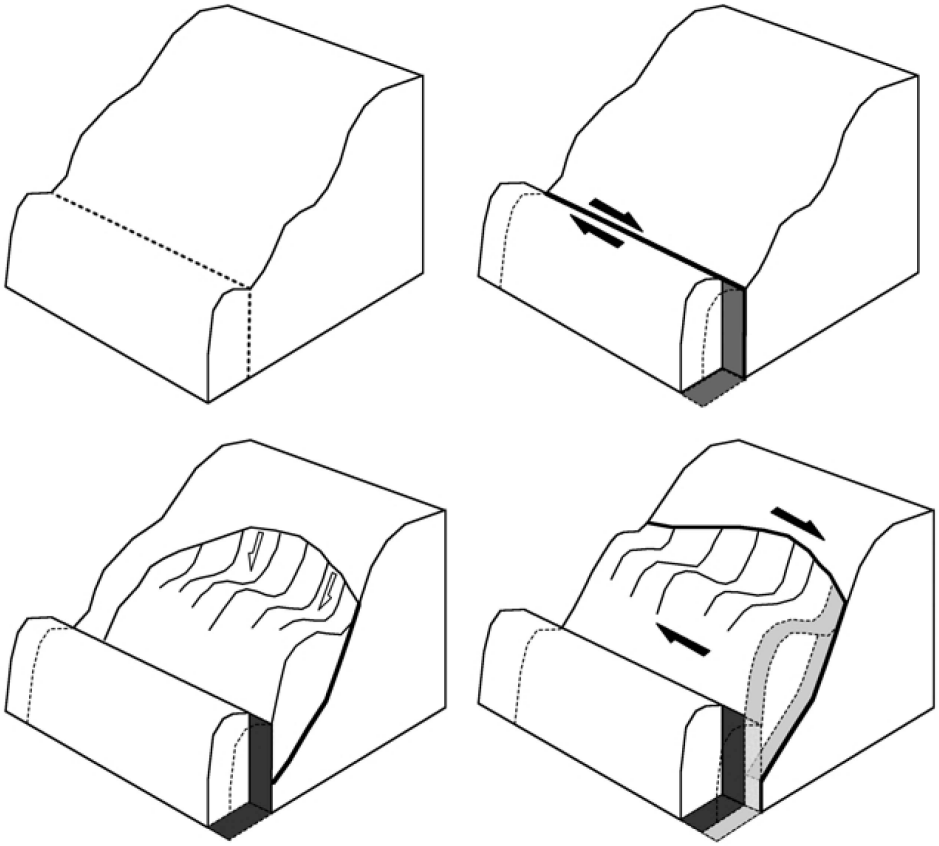

Fig. 9: Schematic model of the interaction between coseismic slip and slop failure a) Primary strike slip-fault in interseismic phase crossing the flank of a ridge b) Right-lateral offset along a strike-slip fault at the flank of a ridge. c) As a result of the earthquake the slope can no longer maintain its stability resulting in a landslide. d) The down-slope push on soil mass that is detached farther upslope on the ridge causes the main trace to become locked. The sub-parallel trending trace formed by the landslide accommodates the horizontal displacement farther upslope.

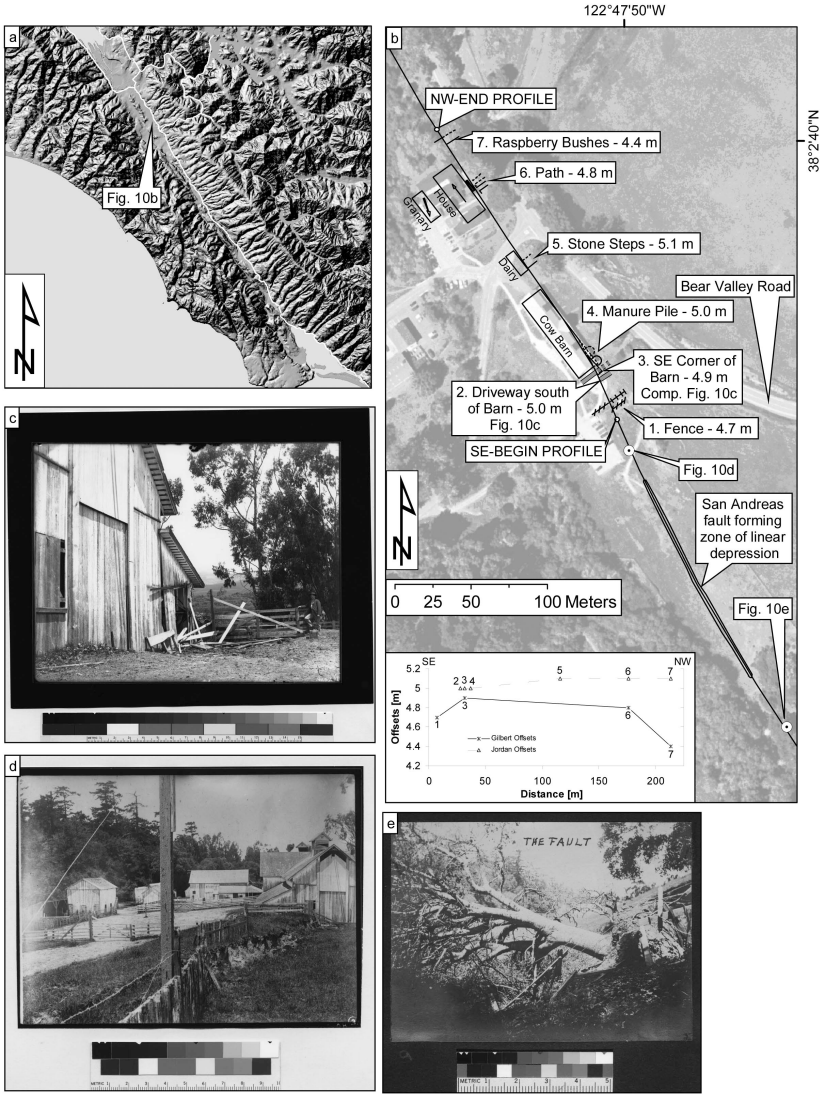

Figure 10

Fig. 10: Historical photographs and measured offsets at the Skinner Ranch. a) Location map. b) Aerial photograph with an overlay of the modified sketch map from G.K. Gilbert that appeared in the Lawson Report (1908). The map also contains compiled information of offset measurements obtained by D.S. Jordan (1907). Using relocated photographs we can identify these location on Gilbert's sketch in Lawson (1908). Numerous features were offset by the 1906 fault trace and have a range of displacements between 4.4-5 m. c) Historical photograph of the offset barn. Legend with photo reads: "The southeast corner of the barn moved northwest to its present position from post on man's foot" (Photo courtesy of Bancroft Library). d) Historical photograph of the offset barn. Legend with photo reads: "Fault rift with scarp and oblique effect of fence, just south of barn on Skinner Ranch" (Photo courtesy of Bancroft Library). The northeast-facing scarp is formed as the ridge is translated northwest. e) Historical photograph of toppled oak tree. Legend with photo reads: "The fault (toppled tree and damaged fence. Marin County.)" (Photo courtesy of Bancroft Library). This fence, which is no longer extant, has been reconstructed as part of the park's "Earthquake Trail" exhibit (Hall, 1974; 1976). The offset of the fence was not measured after the earthquake.

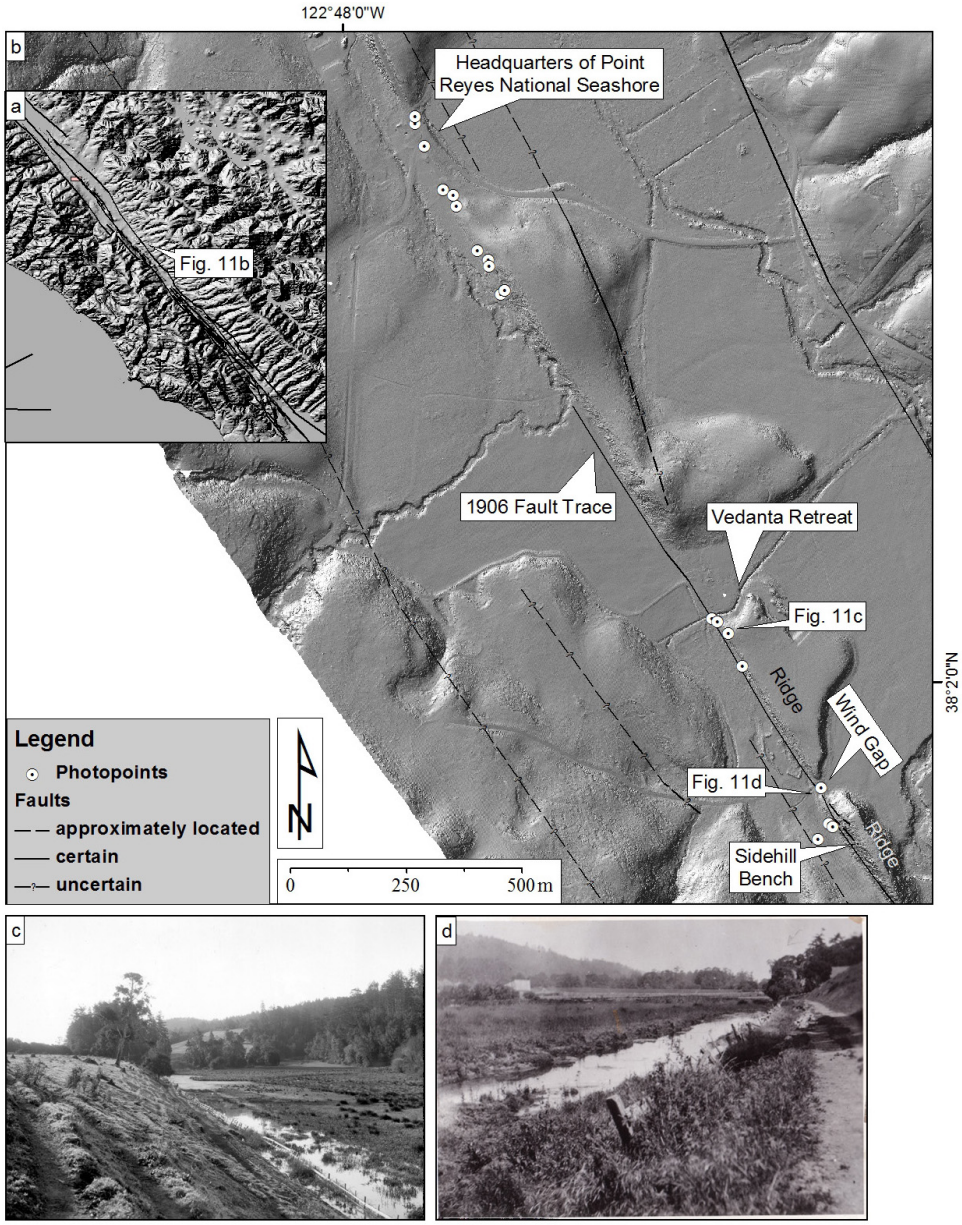

Figure 11

Fig. 11: a) Shaded relief map of Olema Valley and San Andreas fault zone. b) Aerial photograph showing the location of photo relocation points from both the Skinner Ranch, now the Bear Valley Visitor Center and Headquarters of Point Reyes National Seashore, and on the Shafter Ranch, now the Vedanta Retreat in Olema. c) G.K. Gilbert photograph looking southeast along the fault trace showing water forming a pond along the fault on the Shafter Ranch. "California earthquake. Rift topography south of Shafter's place, Olema. A deep fault sag has been aggraded and contains a swamp. The trench occupied by water is part of the trace of the earthquake fault of 1906. Marin County. California, ca. 1906." (Photo 3046, U.S.Geological Survey Archive). d) J.C. Branner photograph of the 1906 fault traced viewed toward the northwest showing slump failure of the road, tilted fence, and a lane of water along the fault rupture in the marsh on the Shafter Ranch (Courtesy of the Stanford University Archives).

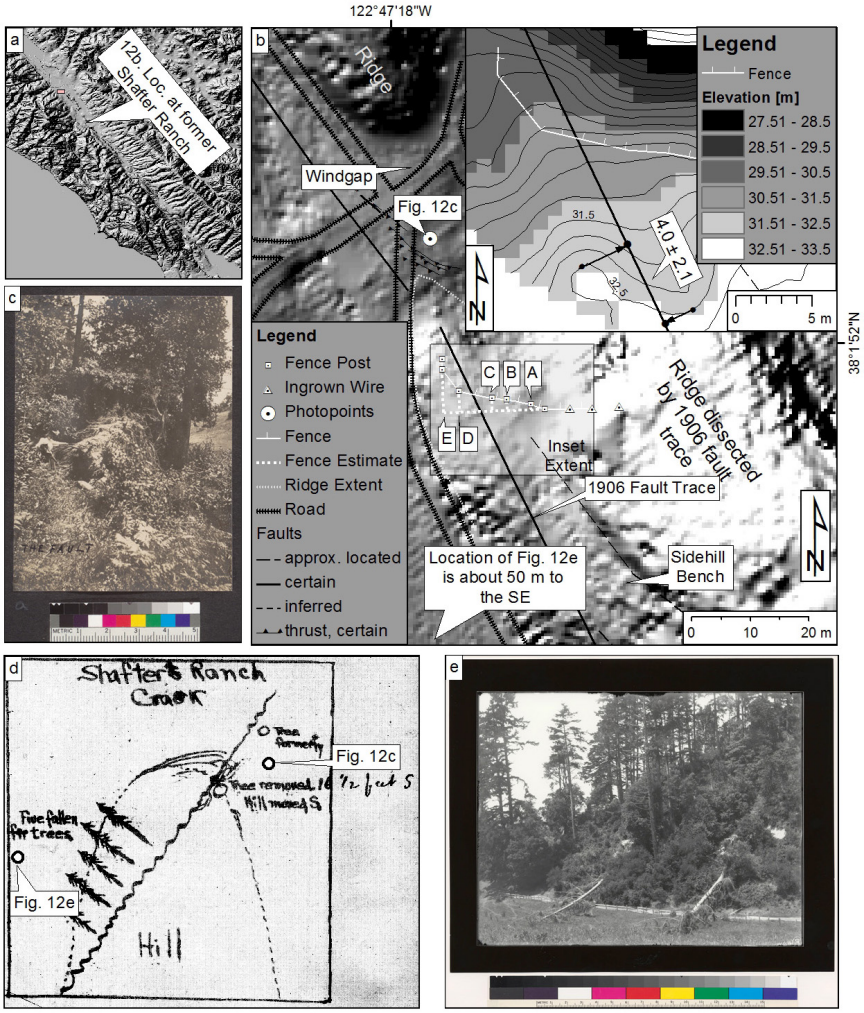

Figure 12

Fig. 12: a) Shaded relief map of Olema Valley showing the location of the Vedanta site. b) LiDAR DEM with an overlay of a kriged surface interpolation of data collected during a real-time kinematic GPS survey of the Vedanta wind gap site. The ridge slice west of the fault and southeast of the wind gap has been translated northwest along the fault trace. The figure shows an offset recorded in a displaced fence. Based on fence posts east of the fault we inferred the original extent of the fence. We measured the following displacements at 5 points based on the estimation of the original fence extent and in-situ observed fence posts: (A) 1.0 m; (B) 1.9 m; (C) 2.2 m, (D) 3.7 m, (E) 7.4 m. The fence forms a bend and reaches its maximum deflection at its westernmost extent. Although the fence was fallen we were able to survey some of the posts on the ground. Towards the east the fence wire was deeply grown into the some trees. c) Historical photo of the translated ridge slice viewed toward the southeast. The image shows a woman standing next to an uprooted tree. View towards the southwest (Courtesy of the Bancroft Library, U.C. Berkeley). d) David Starr Jordan's sketch map of the 1906 fault trace and offset tree on the Shafter Ranch (now the Vedanta Retreat). Jordan did not mark the juxtaposed position west of the fault as the pre-earthquake location of the tree. It is shown as "tree formerly" and was measured to be a 5 m (16.5 foot) offset. Also note the location of "five fallen fir trees" on the ridge to the southeast (Courtesy of the Stanford University Archives). e) Historical photograph of the fallen fir trees as seen on the D.S. Jordan sketch in Figure 12d (Courtesy of the Bancroft Library, U.C. Berkeley).